Published online 12 October 2011 *Nucleic Acids Research, 2012, Vol. 40, No. 3* ***1033–1049***
doi:10.1093/nar/gkr849

Yin Yang 1 contains G-quadruplex structures in its promoter and 5′-UTR and its expression is modulated by G4 resolvase 1

Weiwei Huang[1,2], Philip J. Smaldino[1], Qiang Zhang[1], Lance D. Miller[1], Paul Cao[1], Kristin Stadelman[1], Meimei Wan[1], Banabihari Giri[1], Ming Lei[2], Yoshikuni Nagamine[3], James P. Vaughn[1], Steven A. Akman[1] and Guangchao Sui[1,*]

[1]Department of Cancer Biology and Comprehensive Cancer Center, Wake Forest University School of Medicine, Winston-Salem, NC 27157, USA, [2]Shaanxi Key Laboratory for Molecule Biology of Agriculture, College of Life Sciences, Northwest A&F University, Yangling, 712100 Shaanxi Province, P. R. China and [3]Friedrich Miescher Institute for Biomedical Research Norvartis Research Foundation, 4058 Basel, Switzerland

Received November 23, 2010; Revised September 21, 2011; Accepted September 22, 2011

ABSTRACT

Yin Yang 1 (YY1) is a multifunctional protein with regulatory potential in tumorigenesis. Ample studies demonstrated the activities of YY1 in regulating gene expression and mediating differential protein modifications. However, the mechanisms underlying YY1 gene expression are relatively understudied. G-quadruplexes (G4s) are four-stranded structures or motifs formed by guanine-rich DNA or RNA domains. The presence of G4 structures in a gene promoter or the 5′-UTR of its mRNA can markedly affect its expression. In this report, we provide strong evidence showing the presence of G4 structures in the promoter and the 5′-UTR of YY1. In reporter assays, mutations in these G4 structure forming sequences increased the expression of Gaussia luciferase (Gluc) downstream of either YY1 promoter or 5′-UTR. We also discovered that G4 Resolvase 1 (G4R1) enhanced the Gluc expression mediated by the YY1 promoter, but not the YY1 5′-UTR. Consistently, G4R1 binds the G4 motif of the YY1 promoter *in vitro* and ectopically expressed G4R1 increased endogenous YY1 levels. In addition, the analysis of a gene array data consisting of the breast cancer samples of 258 patients also indicates a significant, positive correlation between G4R1 and YY1 expression.

INTRODUCTION

Yin Yang 1 (YY1) is a multifunctional protein that is essential to differential epigenetic regulation of gene expression and protein modifications. As a ubiquitously expressed protein, YY1 acts as a transcription factor to either activate or repress its target genes depending on the context of its recruited cofactors (1–3). Structural and functional studies indicate that YY1 uses distinct domains to bind to target promoters and recruit transcriptional cofactors to modulate gene expression (4). Many YY1-interacting proteins possess activities of regulating protein modifications. Therefore, YY1 potentially mediates the modifications of a variety of histone and non-histone proteins to determine the expression statuses of its target genes. Consistently, YY1 has been reported to regulate many genes whose products play essential roles in cell proliferation and differentiation [reviewed in (2–5)].

Many lines of evidence suggest a regulatory role of YY1 in cancer development. YY1 is one of the polycomb group (PcG) proteins that are essential contributors to the aberrant epigenetics in cancers (6). At the transcriptional level, YY1 regulates the expression of many cancer-related genes, such as c-Myc, c-fos, erbb2, p53, Rb and cdc6 (7–12), as well as histones H3 and H4 (13,14). During apoptosis, YY1 colocalizes with p53, binds to a subset of p53 DNA-target sites and regulates p53-dependent transcription (15). At the post-translational level, YY1 associates with many proteins with critical regulatory functions, such as p300, HDAC1,2,3, Ezh1, Ezh2, PRMT1, p53, Mdm2, p14ARF, Rb and mTOR (16–25). YY1 is

*To whom correspondence should be addressed. Tel: +1 336 713 0052; Fax: +1 336 716 0255; Email: gsui@wakehealth.edu

The authors wish it to be known that, in their opinion, the first three authors should be regarded as joint First Authors.

essential to the histone methylation mediated by Ezh2 (on H1-K26 and H3-K27) (20,26) and PRMT1 (on H4-R3) (21). We and others demonstrated that YY1 negatively regulates p53 through enhancing Mdm2-mediated p53 ubiquitination and degradation (22,27–29). YY1 also blocks p300-mediated p53 acetylation (27) and inhibits p53-activated transcription (15). Actually, blocking p53 acetylation can both decrease its transcriptional activity (30–32) and facilitate Mdm2-mediated p53 ubiquitination and degradation (33). Therefore, the activities of YY1 in enhancing p53 ubiquitination and inhibiting p53 acetylation converge to the same consequence: antagonizing p53. These multiple functions and unique properties endow YY1 with a pivotal role in epigenetic regulation, including genomic imprinting and chromatin remodeling. Consistently, YY1 is highly expressed in human breast cancer (9), prostate carcinoma (34), acute myeloid leukemia (35), osteosarcoma (36,37) and cervical cancer (38).

Limited research has been carried out to investigate the mechanisms underlying how YY1 is regulated. YY1 gene expression can be stimulated by different growth stimuli, including insulin-like growth factor-1, fibroblast growth factor-2 and morphine. Factors that inhibit YY1 expression include prohibitin, microRNA-29, DETANONOate (a nitric oxide donor) and naloxone [see review (3)]. YY1 may also self-regulate its own expression through binding to the intron 1 (39).

G-quadruplex (G4) is a four-stranded secondary structure of DNA or RNA stabilized by Hoogsteen hydrogen bonding of guanine quartets and the stacking of these planar quartets. A genome-wide survey of the evolutionary conservation of DNA motifs indicated that G4 DNA motifs are significantly conserved (40). Increasing evidence suggests an important role of G4 DNA structures in regulating gene expression (41). Interestingly, G4 DNA structures are more enriched in promoters than other regions of genomic DNA, especially in genes involved in development, survival and proliferation.

Recent studies implicate a role for G4 DNA in tumorigenesis. The telomeric G-rich DNA overhang forms G4 structures that inhibit the activity of telomerase required for the immortalization of most cancer cells (42). The majority of proto-oncogenes possess G-rich promoters, while promoters of tumor suppressors are diminished of closely linked G-runs, relative to the genomic average (43). Consistently, G4 DNA structures have been demonstrated to regulate the expression of a number of well-characterized oncogenes, such as c-Myc, K-RAS, Bcl-2 and hTERT. Actually, the six critical cellular and microenvironmental processes that are aberrantly regulated in oncogenic transformation, as summarized by Hanahan and Weinberg (44), are all modulated by genes that are regulated by G4 structures (40).

Several DNA and RNA helicases with the catalytic activity to unwind or resolve G4 DNA or G4 RNA structures have been identified, including BLM, WRN, FANCJ, G4R1 (or G4R1/RHAU, DHX36), RNA helicase II (DHX9) and SV40 large T-antigen (45–47). These G4 DNA or RNA resolvases can unwind the four-stranded G4 structures to a single-stranded form in an ATP-dependent fashion (48,49). Among them, G4R1 possesses tetramolecular and intramolecular quadruplex G4 DNA and G4 RNA resolving activity (50–52). Importantly, G4R1 has been observed to be increasingly expressed in cancers (unpublished data from Akman group), suggesting its regulatory role in promoting the expression of oncogenes.

Based on previous studies of YY1 in differential cancer-related processes, we concluded that YY1 likely plays an oncogenic or proliferative role in tumorigenesis (3). A previous study indicated that the promoter of mouse YY1 is G/C rich (53). Therefore, we analyzed the primary sequences at the upstream of the human YY1 coding region, and observed the presence of multiple G- or C-rich strings. In this report, we demonstrate that G4 structures are formed by the oligonucleotides whose sequences are found in the promoter and 5′-untranslated region (UTR) of YY1. The alteration of these sequences affects the expression of a reporter gene. G4R1 promotes the expression driven by the YY1 promoter, but not that mediated by the YY1 5′-UTR. Consistently, ectopic G4R1 increases the endogenous YY1 levels and G4R1 expression positively correlates with YY1 in the samples from 258 breast cancer patients. Overall, our data reveal the presence of G4 structures in the YY1 promoter and 5′-UTR, and suggest that G4R1 may modulate YY1 expression by resolving G4 DNA structure in the YY1 promoter.

MATERIALS AND METHODS

Cell culture and transient transfection

HeLa and 293T cells were cultured in Dulbecco's modified Eagle's medium containing 10% fetal bovine serum. Lipofectamine 2000 was used in transient transfection. The HeLa cells expressing doxycycline-inducible G4R1 shRNA were reported previously (54) and the induction was achieved by adding a final concentration of 1.5 μg/ml doxycycline in the medium.

Antibodies and oligonucleotides

YY1 antibody (H-10), histone H3 antibody (FL-136) and non-specific mouse IgG (sc-2343) were purchased from Santa Cruz Biotechnology. Mouse monoclonal G4R1/RHAU antibody (12F33) was generated against a peptide corresponding to the amino acids 991–1007 of G4R1, as previously described (55). β-Actin antibody was from Chemicon International Inc. DNA oligonucleotides or primers were synthesized by Bioneer Inc. and Integrated DNA Technologies (IDT), while the RNA oligonucleotides were made by the Biomolecular Resource Laboratory, Wake Forest University School of Medicine. The annealing condition for G4 structure formation followed a published procedure (52) with modifications (Supplementary Figure S1).

DNA vector construction

To generate reporter constructs driven by the YY1 promoter, the −1703 to −1 (with the transcription start

site designated as +1; this applies to all following descriptions) of the YY1 promoter region was amplified by PCR using AccuPrime Pfx DNA polymerase (Invitrogen) with primers F1: 'cctg gaattc att ggt gtt tat ggg gaa gta tca' and R1: 'ctag tctaga ctc gat tct cct ctc ggc caa tc' (F: forward; R: reverse). The template was the clone RP11-459E8 containing YY1 gene purchased from the BACPAC Resources Center (Oakland, CA, USA). The PCR fragment was digested by EcoRI and XbaI (underlined in the primer sequences) and inserted into EcoRI and NheI digested pGluc Basic (New England BioLabs Inc.), of which the multiple cloning site has been modified. To mutate the G4 structure-forming sequence between −409 and −347 in the negative strand of the YY1 promoter, we synthesized two primers F2: 'ccgtg gcatgc gcc tca acc tcg ctc ccg gcc ggc ccc tc' and R2: 'ccgtg gcatgc gcg gcc cgg ggg ccg cgc ggg gag' containing a created SphI sites (underlined) that facilitated the DNA subcloning and altered the guanines essential to the predicted G4 structure formation. They were respectively used with the first two primers (F1 with R2; F2 with R1) to amplify the YY1 promoter as two PCR fragments that were then digested by the corresponding restriction enzymes and subcloned simultaneously into the modified pGluc Basic vector. As a result, the mutated form of the YY1 promoter containing an altered G4 structure-forming sequence was generated.

To study the contribution of the G4 structure forming sequence in the YY1 5′-UTR to Gluc expression, we amplified the YY1 5′-UTR using primers F3: 'cacg acgcgt agg gcg aac ggg cga gtg gca g' and R3: 'cgag ggatcc ggc tga ggg ctc cgc cgc cac g' with the RP11-459E8 plasmid as a template. After the digestion of MluI and BamHI (underlined), the fragment was inserted between the PGK promoter and Gluc cDNA of a reporter construct. To mutate the G4 structure-forming sequence in the YY1 5′-UTR, we synthesized two additional primers F4: 'cgga ggtacc cgg gga agc ccc gcc gcc gcc' and R4: 'cgga ggtacc tcg cct cgg tgc gcc cgc gcc' that both contain a created KpnI sites to facilitate the subcloning and mutate the guanines essential to the predicted G4 structure formation. The PCR reactions using these primers F3 with R4 and F4 with R3 amplified the YY1 5′-UTR into two fragments, which were then simultaneously subcloned into the pPGK-Gluc vector. The sequences of all wild-type and mutated reporter constructs described here were confirmed by DNA sequencing.

Circular dichroism study

To anneal G-quadruplexes, 20 µl of 100 pmol/µl DNA or RNA oligonucleotides was mixed with 180 µl of TE buffer (10 mM Tris–HCl, 0.1 mM EDTA, pH 7.5) and annealed as described in Supplementary Figure S1. These annealed oligonucleotides were diluted to 4 µM in the TE buffer supplied with 50 mM KCl. Circular dichroism (CD) spectra were recorded on a spectropolarimeter (Aviv Model 202 CD Spectrometer, equipped with a thermoelectrically controlled cell holder) using a quartz cell of 0.5 mm optical path length, and over a wavelength range from 200 to 350 nm at 25°C. For melting temperature scan, we used a temperature range from 20°C to 95°C with a constant wavelength of 262 nm. The CD spectra were presented with the subtraction of the signal contributed by the buffer.

5′-^{32}P-end labeling of G4 nucleic acids

To produce a 5′-^{32}P-labeled G4 oligonucleotide, an aliquot (<1/10 of the final volume for the labeling reaction) of the annealed G4 oligonucleotide was incubated with T4 polynucleotide kinase (Promega Corp.) and γ-^{32}P-ATP for 30 min at 37°C, according to the manufacturer's instructions. The 5′-^{32}P-labeled G4 oligonucleotides were purified with a MicroSpin G25 column (GE Healthcare) equilibrated with TEK buffer (10 mM Tris, 1 mM EDTA and 50 mM KCl) and stored at −20°C.

Dimethyl sulfate footprinting

Dimethyl sulfate (DMS) footprinting was carried out following a modified version of previously published protocols (56,57). A purified 5′-^{32}P-labeled oligonucleotide was annealed in the absence and presence of 100 mM KCl or 100 mM LiCl, and 1 µg/µl of sonicated salmon sperm DNA. DMS (Sigma) dissolved in ethanol (DMS:ethanol, 4/1, v/v) was added to the oligonucleotide solution (0.7 µl to a total volume of 49 µl) and incubated at room temperature for 3 min. The reaction was stopped by adding two volumes of the stop solution (1.5 M sodium acetate, pH 7.0, 1.0 M β-mercaptoethanol and 0.5 µg/µl tRNA). The DNA was precipitated with four volumes of ethanol and resuspended in 1.0 M piperidine (Sigma). After cleavage at 95°C for 30 min, the DNA was precipitated by adding 20 µg of glycogen (Invitrogen), one-ninth volume of 3 M sodium acetate (pH 5.2) and two volumes of ethanol. For the Maxam-Gilbert chemical G+A sequencing reaction, an oligonucleotide was treated by formic acid and piperidine following a standard protocol (58). The samples were resuspended in 90% formamide and 20 mM EDTA, denatured at 95°C for 3 min and run for 2–3 h on an 18% denaturing polyacrylamide gel (Bio-Rad) in 1× TBE and 8.0 M urea. After the electrophoresis, the gel was fixed in a solution containing 50% methanol and 10% polyethylene glycol 400, and dried at 80°C for 3 h followed by autoradiography.

In vitro DNase I footprinting of the YY1 promoter regions

As previously demonstrated by Sun *et al.* (59,60), the G4 structures and i-motifs formed by G-rich and C-rich regions, respectively, are resistant to DNase I cleavage. The experiments followed the procedure described by Sun (60). We first subcloned a fragment (−1180 to −329) of the YY1 promoter into pGL3-Basic vector (Promega) between HindIII and XhoI sites. The generated vector pGL3/YY1-short-prmt included the G4 structure forming or the YP-3 sequence (−409 to −347). This plasmid (2 µg in 25 µl) was incubated at 37°C overnight in 50 mM Tris–HCl, pH 7.6 in the absence or presence of 100 mM KCl. The sample was then mixed with 2 µl of 0.1 U/µl DNase I and incubated at ambient temperature

for 2 min, immediately followed by DNA precipitation and primer extension reaction using ^{32}P-labeled primer P1 (CTT TCT TTA TGT TTT TGG CGT CTT) located downstream of the inserted YY1 promoter fragment and Thermo Sequenase (Affymetrix Inc.). Meanwhile, the G-rich negative strand of the YY1 promoter fragment in the untreated plasmid was sequenced by the same primer using Thermo Sequenase Cycle Sequencing Kit (Cat# 78500, Affymetrix Inc.) following the procedure provided by the manufacturer. These samples were resolved by a 6% denaturing polyacrylamide gel (Bio-Rad) in 1× TBE and 8.0 M urea at constant 55 W for 3 h. After the electrophoresis, the gel was dried at 80°C for 2 h followed by autoradiography.

Electrophoretic mobility shift assays

Recombinant G4R1 purified as described previously (50) at concentrations of 10–120 pM was incubated with 1 pM of 5′-^{32}P-labeled G4 nucleic acid in RES–EDTA buffer (100 mM KCl, 10 mM NaCl, 3 mM $MgCl_2$, 50 mM Tris–acetate, pH 7.8, 70 mM glycine, 0.012% bovine α-lactalbumin, 10% glycerol, 10 mM EDTA) at 37°C for 30 min. Binding mixtures were then analyzed by 10% non-denaturing polyacrylamide gel. Electrophoresis was performed at 70 V for 10 h in a cold room. Gels were imaged on a Typhoon 9210 Imager (GE Healthcare). The experiments determining the effect of ATP on G4R1/YP-3 association were carried out as previously described (61). An amount of 1 pM of 5′-^{32}P-labeled self-annealed YP-3 was incubated with different amounts (25, 75 and 300 pM) of G4R1 in the presence and absence of 5 mM ATP at 37°C for 30 min. The samples were analyzed on 10% non-denaturing polyacrylamide gel at 55 V for 18 h, followed by the same imaging procedure described above.

Reporter assay

293 T cells cultured in 24-well plates were transfected with 200 ng of the reporter constructs containing the YY1 promoter, 5′-UTR or their mutant forms with altered sequences in the potential G4 structure-forming sequences, and 2 ng of a control plasmid pCMV/SEAP (secreted alkaline phosphatase). To detect the effect of G4R1 on the YY1 promoter or 5′-UTR, 500 ng of G4R1 expression plasmid or empty vector was cotransfected with 200 ng of reporter plasmid and 2 ng of pCMV-SEAP plasmid. Aliquots of medium from the transfected wells were collected 48 h post-transfection to measure Gaussia luciferase (Gluc) activity then normalized against the SEAP activity in the same sample, according to the procedure described by us (62). Each condition was tested in triplicate and repeated over three times.

Chromatin immunoprecipitation assay

Chromatin immunoprecipitation (ChIP) assays were performed as previously reported (63). Samples immunoprecipitated by a control IgG, G4R1 antibody and histone H3 antibody were analyzed with Real-Time PCR using the FastStart Universal SYBR Green Master (Roche Diagnostics GmbH) and the primers F5: 'ccc gaa gcc agg cga caa gaa c' and R5: 'gtg caa cag cca caa aac ccg'. The F5 and R5 are located at the upstream (−525) and downstream (−208) of the potential G4R1-binding site, respectively, in the YY1 promoter. As a control, we also designed two primers F6: 'atg cta agg cca aaa aca acc agt g' and R6: 'tga aac gag att aca gag caa gat a' that are located in the YY1 exon 5 (+1700 and +1948, respectively) and amplify a fragment with relatively low G/C contents (34.6% of G/C; 17.3% of each).

Microarray analysis of YY1 and G4R1 expression profiles

The Uppsala breast cancer cohort with the tumor samples from 258 breast cancer patients (64) profiled on the Affymetrix U133A and U133B GeneChips were accessed via the caArray website (https://array.nci.nih.gov/caarray/project/details.action?project.experiment.publicIdentifier=mille-00271), accession id: mille-00271. The microarray data were MAS5.0 normalized by scaling the mean of each array to a target signal intensity of 500 and log (base 2) transformed. Multiple correlated probe sets corresponding to YY1 and G4R1 (or DHX36) were identified. Three YY1 probe sets (U133A: 213494_s_at, 201901_s_at and 200047_s_at) and three G4R1 probe sets (U133B: 223138_s_at, 223139_s_at and 223140_s_at) were averaged together to represent expression profiles of YY1 and G4R1, respectively. The correlation of YY1 to G4R1 expression was evaluated by Pearson correlation using SigmaPlot 11.0 software.

Statistical analysis

All data in reporter assays and qPCR are presented as mean ± SD. Comparisons between two groups on a single parameter were conducted using Student's *t*-test. Statistical analyses were performed using KaleidaGraph. The criterion for statistical significance was set at $P < 0.05$.

RESULTS

The YY1 promoter and 5′-UTR are highly G/C-rich and contain potential G4 DNA and G4 RNA structure-forming sequences, respectively

For a specific gene, G4 DNA structure can be formed by either the positive or the negative strand of its promoter, while G4 RNA structure in the 5′-UTR will only be present in the mRNA coded by the positive strand. Thus, the G/C content in a promoter and G content in a 5′-UTR are essential determinants to the formation of G4 DNA and G4 RNA motifs, respectively. A previous study by Seto's group demonstrated that the promoter region within 1500-bp upstream of human YY1 transcription start site did not show marked difference in reporter assays compared to the fragment up to −3600 bp (65). Therefore, we first analyzed the G/C contents in different promoter regions from the YY1 transcription start site (designated as +1) up to its 1500-bp upstream (−1500), and the 5′-UTR of the YY1 mRNA. As shown in Figure 1A, the G/C contents of the YY1 promoter increase monotonically as the analyzed region gets closer to the transcription start site. Remarkably, the G/C

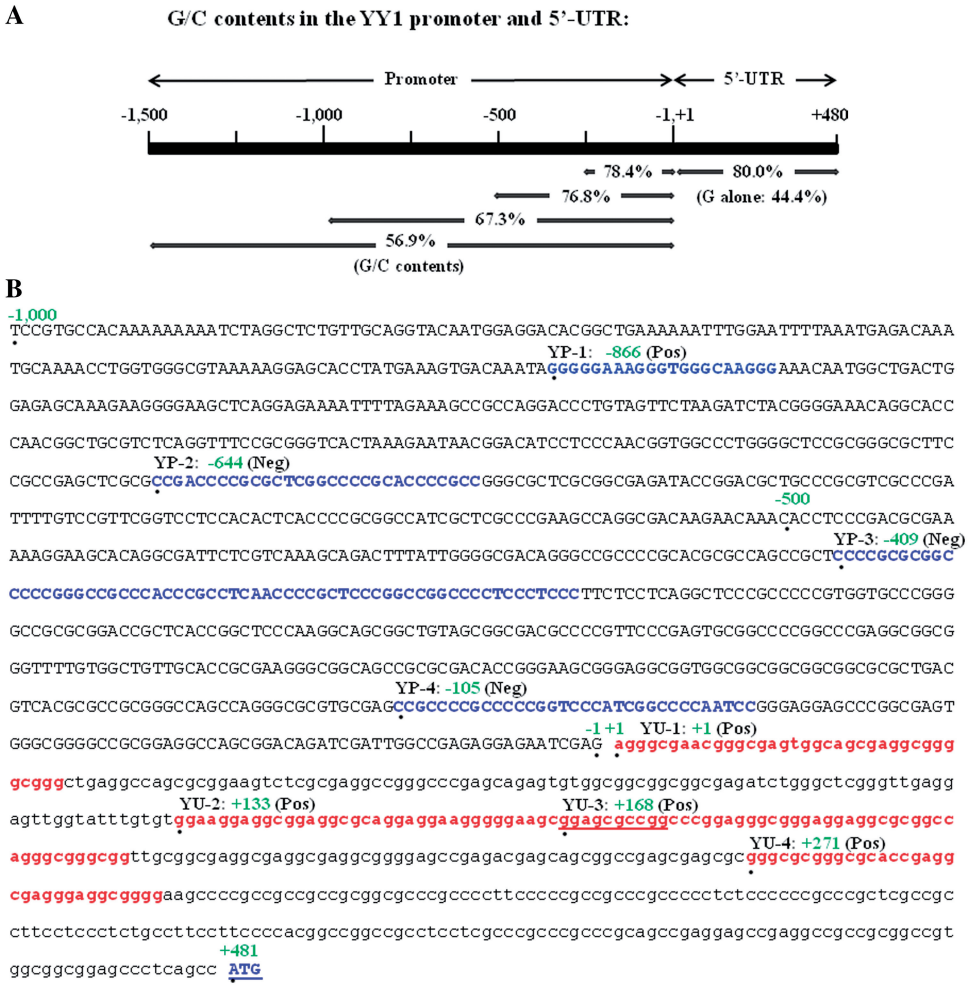

Figure 1. Schematic primary structure and sequence of the YY1 promoter and 5′-UTR. (**A**) Primary structure and the G/C contents of the YY1 promoter and 5′-UTR. The percentages of G/C contents in the 1500 bp-YY1 promoter and the 5′-UTR, as well as the G content in the 5′-UTR, are indicated. The transcription start site is designated as '+1'. (**B**) The DNA sequence of the YY1 promoter (1000 bp) and 5′-UTR. The G4 DNA candidates in the YY1 promoter, either the positive or negative strands, are in blue text, while the G4 RNA candidates in the YY1 5′-UTR are in red text. The promoter is shown in capital letters, while the 5′-UTR is in lower case. YP-1, -2, -3 and -4 in the YY1 Promoter (YP) and YU-1, -2, -3 and -4 in the YY1 5′-UTR (YU) indicate the positions of the oligonucleotides shown in Figure 2A. The numbers in green text indicate the positions of the first nucleotides in these candidate G4 structure-forming sequences, which are identified by the dots beneath them. The underlined sequence in the YY1 5′-UTR is the overlapped region of YU-2 and YU-3. Neg: negative strand; Pos: positive strand.

content from −500 to −1 is >76.8%. The G/C content in the YY1 5′-UTR is 80.0%, with a G content of 44.4%, markedly higher than the average of the four nucleotides. These analyses clearly indicate that YY1 has great potential of containing G4 motifs in its promoter and 5′-UTR regions.

Since the G/C content from −1000 to −1 in the YY1 promoter is >67.3%, we chose to analyze this region for potential G4 DNA structure-forming sequences based on the algorithm proposed in previous literature (66). As a result, we identified four elements (YP-1 to YP-4; YP: YY1 Promoter) that may form G4 DNA structures on either the positive strand (YP-1) or negative strand (YP-2, -3 and -4) of the YY1 promoter (blue text in Figure 1B). The analyses of the YY1 5′-UTR also revealed four candidate sequences (YU-1 to YU-4; YU: YY1 5′-UTR) for G4 RNA structure formation (red text in Figure 1B).

Analyses of oligodeoxyribonucleotides derived from the YY1 promoter and 5′-UTR by CD spectroscopy indicate the formation of G4 structures

To examine G4 DNA or RNA structure formation by the candidate sequences in the YY1 promoter and 5′-UTR shown in Figure 1B, we designed oligodeoxyribonucleotides based on either their original or complementary sequences (Figure 2A). For the candidates in the YY1 5′-UTR, we planned to use their sequences to make oligodeoxyribonucleotides in this primary screening analysis based on the structural similarity between G4 DNA and G4 RNA, and then confirm the presence of G4 RNA structure using the oligoribonucleotides. We individually annealed these oligonucleotides as described in Supplementary Figure S1. As a control, we also synthesized a sequence located in the human c-Myc promoter that forms a well-characterized G4 DNA

structure (c-Myc G4 DNA, Figure 2A) (67). These annealed samples were then analyzed by CD spectroscopy.

In all CD studies, the annealed c-Myc G4 oligodeoxyribonucleotide displayed peaks of positive molar ellipticity at 262 nm and negative molar ellipticity at 240 nm, which is characteristic of a parallel G4 structure (68). Oligodeoxyribonucleotides YP-3 and YU-4 displayed peaks of positive molar ellipticity at 262 nm (closed triangles, Figure 2B), indicative of the presence of a parallel G4 structure in this *in vitro* condition. However, a second peak of positive molar ellipticity at 295 nm was also observed with both oligodeoxyribonucleotides, suggesting the presence of a G4 structure with anti-parallel strands. To confirm that these signature peaks indicate G4 structure, we synthesized two control oligodeoxyribonucleotides YP-3M and YU-4 M, in which the guanines with predicted roles in G4 structure formation of YP-3 and YU-4 were replaced by adenines (Figure 2A). These mutated oligonucleotides exhibited altered CD spectra with a single peak not coincident with either the 262 or 295 nm peaks observed with the wild-type oligodeoxyribonucleotides (open triangles, Figure 2B). These results indicate that the oligodeoxyribonucleotides YP-3 and YU-4 form G4 structures with a mixture of parallel and anti-parallel strands.

The spectra of the other three oligodeoxyribonucleotides YP-1, YP-2 and YP-4 whose sequences are found in the YY1 promoter gave no indication of G4 structure (Figure 2B). Among the other three oligodeoxyribonucleotides whose sequences are located in the YY1 5′-UTR, the CD spectra of YU-1 and YU-2, but not YU-3, were similar to that of YU-4, although the peak heights of the YU-2 spectrum were substantially diminished (Figure 2B), suggesting that these two oligodeoxyribonucleotides can also form G4 structures with a mixture of parallel and anti-parallel strands.

DMS footprinting assays of YY1 G4 DNA structures

The YP-3 oligonucleotide contains 7–9 separate G-runs (Figure 2A). To determine whether YP-3 forms intramolecular or intermolecular structures, we carried out a stoichiometry study. The labeled and unlabeled YP-3 and YP-3-10A (YP-3 with 10 adenines added to its 3′-end) were mixed in different combinations and annealed in the presence of 50 mM KCl, followed by analysis in a 20% non-denaturing polyacrylamide gel. When YP-3

A

Name	Position	Sequence
YP-1*	-865 *to* -845	GGGGGAAAGGGTGGGCAAGGG
YP-2§	-643 *to* -614	CCGACCCCGCGCTCGGCCCCGCACCCCGCC
YP-2*		GGCGGGGTGCGGGGCCGAGCGCGGGGTCGG
YP-3§	-409 *to* -347	CCCCGCGCGGCCCCCGGGCCGCCCACCCGCCTCAACCCCGCTCCCGGCCGGCCCCTCCCTCCC
YP-3*		GGGAGGGAGGGGCCGGCCGGGAGCGGGGTTGAGGCGGGTGGGCGGCCCCGGGGGCCGCGCGGGG
YP-3M*		GaGAGaaAGaaGCCGGCCGaGAGCGaaGTTGAGGCGaGTGaGCGGCCCGaGaGCCGCGCGaaG
YP-4§	-105 *to* -73	CCGCCCCGCCCCCGGTCCCATCGGCCCCAATCC
YP-4*		GGATTGGGGCCGATGGGACCGGGGGCGGGGCGG
YU-1*	+1 *to* +36	agggcgaacgggcgagtggcagcgaggcggggcggg
YU-2*	+133 *to* +177	ggaaggaggcggaggcgcaggaggaaggggaagcggagcgccgg
YU-3*	+168 *to* +214	ggagcgccggcccggagggcgggaggaggcgcggccagggcgggcgg
YU-4*	+271 *to* +303	gggcgcgggcgcaccgaggcgagggaggcgggg
YU-4M*		gAgcgcgAgcgcaccgaggcgagAgaggcgAgg
c-Myc G4 DNA*		GGCCGCTTATGGGGAGGGTGGGGAGGGTGGGGAAGGTGGGGAGGAGACTC
PolyA Zic-1 G4 DNA*		AAAAAAAAAA GGGTGGGGGGGGCGGGGGAGGCCGGGG AAAAAAAAAA
rAGA*		AAAAAAAAAAAAAAAAGGGGGAAAAAAAAAAAAAAA

* The sequences of the synthesized oligonucleotides.
§ The original sequences in the YY1 promoter whose potential G4 structures are present in the negative strands.

Figure 2. The CD and DMS footprinting to determine the G4 structure of the oligodeoxyribonucleotides. (**A**) The sequences of the oligonucleotides for the candidate G4 structure-forming sequences located in the YY1 promoter and 5′-UTR. The oligonucleotide sequences (Asterisk), their original sequences (section symbol) when the potential G4 structures are present in the negative strand (for YP-2, -3 and -4) and their positions are indicated. The guanines that likely contribute to the G4 structure formation are underlined. YP-3M and YU-4M contain the mutated nucleotides (underlined and in reversed cases from the other bases in the same sequences) that are predicted to disrupt the potential G4 structures in YP-3 and YU-4, respectively. The sequences of c-Myc G4 DNA (67), Zic-1 G4 DNA (73) and rAGA G4 RNA (50) have been previously reported. (**B**) CD analyses of the oligodeoxyribonucleotides. The red dashed lines pointed to by the closed arrow heads indicate the signature peaks of parallel G4 structures at 262 nm, while the blue dashed lines pointed to by the open arrow heads indicate the peaks of molar ellipticity after the G4 structure-forming sequences were mutated. (**C**) DMS footprinting assay to confirm the G4 DNA structure in YP-3. The 5′-^{32}P-labeled oligodeoxyribonucleotide YP-3 was annealed under the conditions of no added cation (lane 1), in the presence of 100 mM KCl (lane 2) or 100 mM LiCl (lane 3) and then treated with DMS. The result of formic acid treatment (Maxam-Gilbert G+A reaction) is shown on the left. The dashed lines align the bands with the YP-3 sequence, shown to the right. The markedly protected guanines in lane 2 compared to the other two lines are marked by arrow heads.

(continued)

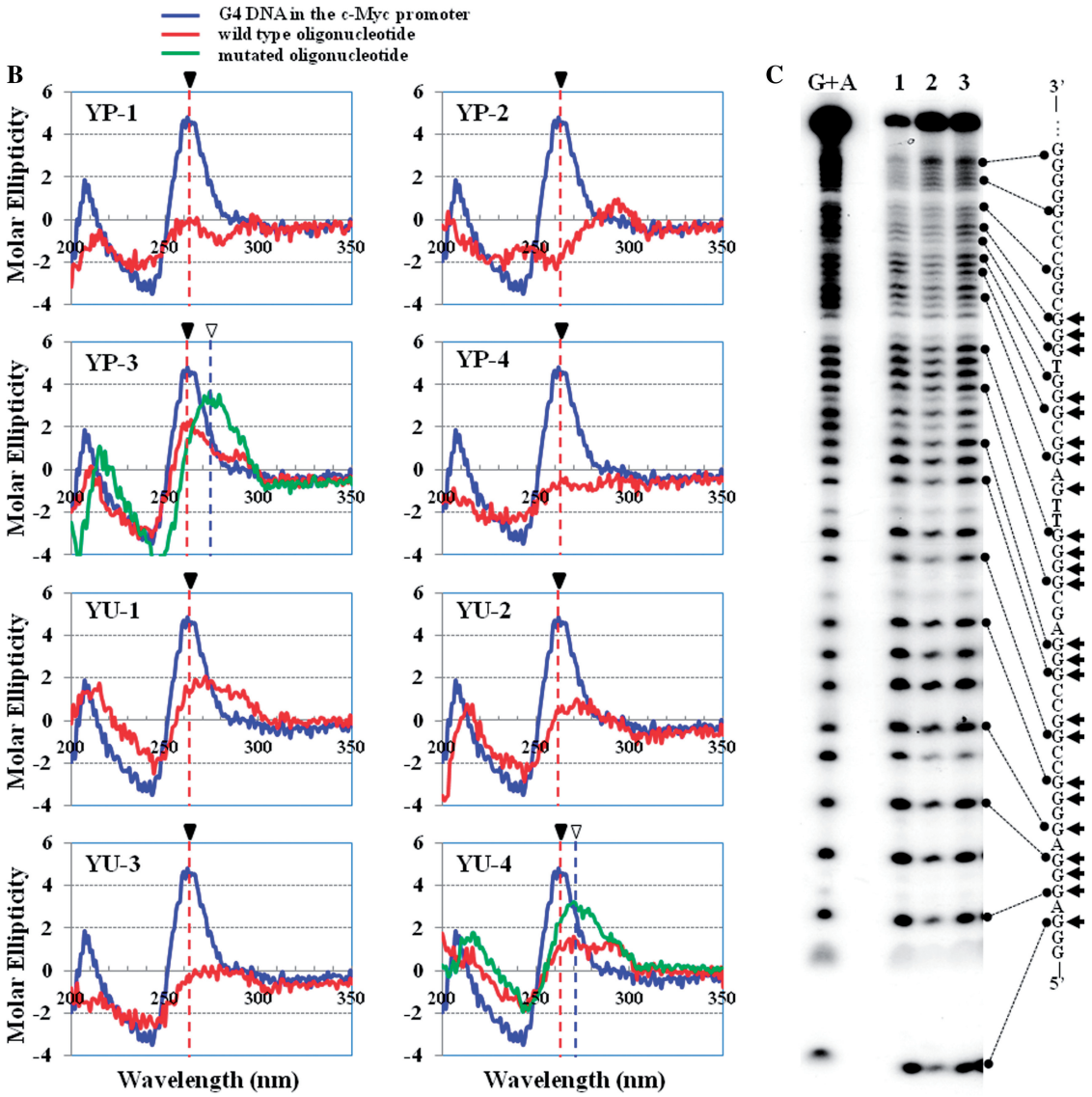

Figure 2. Continued.

and YP-3-10 A were annealed individually, each of them exhibited a major band (lanes 1 and 2, Supplementary Figure S2). When each of them was annealed in the presence of the other oligonucleotide in either unlabeled or labeled status, its major band did not show any shift and no noticeable extra band was detected (lanes 3–7). The oligonucleotides without annealing treatment also showed two major bands migrating to the same positions of their correspondingly annealed samples (lanes 8 and 9), suggesting their instant and favorable transition to the G4-containing structures. Overall, the results of this stoichiometry study strongly suggested that the YP-3 oligonucleotide forms intramolecular, instead of intermolecular, structures.

The guanine N7 in double- and single-stranded DNA is available for methylation by DMS, while the N7 of the guanines in a G4 structure is inaccessible due to the formation of Hoogsteen hydrogen bonds. To confirm the G4 DNA structure in the YY1 promoter and 5′-UTR, we determined DMS-accessibility of the guanine N7 in the oligodeoxyribonucleotide YP1 to YP-4 and YU-1 to YU-4 annealed in the absence and presence of 100 mM KCl or 100 mM LiCl. Among these oligodeoxyribonucleotides, the YP-3 exhibited the most pronounced sensitivity changes to DMS-mediated methylation (Figure 2C and Supplementary Figure S3). Compared to the conditions of no extra cation and 100 mM LiCl, most guanines at the 5′-end of the YP-3 in the presence of 100 mM KCl were markedly protected, indicating the presence of Hoogsteen hydrogen bonds, as would be expected with the formation of G4 DNA structures. This result is consistent with the CD study, strongly indicating the presence of G4 DNA structure in the YY1 promoter. Among other YP-oligodeoxyribonucleotides, the YP-1 and YP-2, but not YP-4, showed partial protection (Supplementary Figure S3A). Since the DMS footprinting result of the

YP-3 was consistent to its CD analysis, we focused on this region for further studies. We also observed partial (YU-4) or marginal (YU-1, -2 and -3) protection of the YU-oligodeoxyribonucleotides to DMS-mediated methylation (Supplementary Figure S3B). However, as an example of a G4 structure located in the YY1 5′-UTR, we only focused on YU-4 for further investigation.

The strong monovalent cation dependence of the formation of secondary structure by oligodeoxyribonucleotide YP-3 and oligoribonucleotide YU-4 confirms the presence of G4 DNA structures

It is known that the formation of G4 structure is stabilized by potassium, but disfavored by lithium ions (69). Therefore, to confirm that oligodeoxyribonucleotide YP-3 and oligoribonucleotide YU-4 self-anneal into G4 structures, we determined the effects of the monovalent cationic environment on the G4 structure formation and thermal stability of the secondary structure formed by these ribonucleotides. We annealed oligodeoxyribonucleotide YP-3 and oligoribonucleotide YU-4 in the absence and presence of 50 mM KCl or 50 mM LiCl, and then carried out CD analyses, again using c-Myc G4 DNA as a control. As shown in the top panels of Figure 3A and B, both wild-type oligodeoxyribonucleotide YP-3 and oligoribonucleotide YU-4, similar to the c-Myc G4 DNA, exhibited peaks of positive molar ellipticity at 262 nm and negative molar ellipticity at 240 nm when annealed in 50 mM KCl. Both the positive and negative peaks of molar ellipticity were markedly diminished when the YP-3 and YU-4 were annealed in 50 mM LiCl, or in a buffer containing no additional monovalent cation. The CD spectra of self-annealed oligodeoxyribonucleotide YP-3M and oligoribonucleotide YU-4M that contain mutated nucleotides in the G4 sequences displayed small peaks of positive and negative molar ellipticity at 262 and 240 nm, respectively, but these peaks displayed no dependence on the local monovalent cation environment (bottom panels in Figure 3A and B). These spectra are consistent with the formation of parallel G4 DNA and RNA structures, respectively, by oligodeoxyribonucleotide YP-3 and oligoribonucleotide YU-4. It is noteworthy that the spectrum of the oligoribonucleotide YU-4 contains no evidence of an anti-parallel G4 structure. This is because the 3′-endo pucker of ribose in RNA is known to cause a prohibitively high energy cost to the anti-syn rotation necessary for anti-parallel G4 structure formation (70,71).

Marked monovalent cation dependence of the thermal stability of secondary structure by oligodeoxyribonucleotide YP-3 and oligoribonucleotide YU-4 confirms the presence of G4 structures

G4 nucleic acids are thermostable structures. Therefore, DNA or RNA sequences with potential of forming G4 structures typically show high melting temperatures (T_{ms}). To further confirm the G4 structures in the oligodeoxyribonucleotide YP-3 and oligoribonucleotide YU-4, we determined the temperature dependence of the positive peak of molar ellipticity at 262 nm for these two oligonucleotides and their mutants annealed in the presence of 50 mM KCl, 50 mM LiCl, or no additional monovalent cation in the temperature range from 20°C to 94°C. As shown in the top panels of Figure 3C and D, wild-type oligodeoxyribonucleotide YP-3 and oligoribonucleotide YU-4 clearly showed higher thermal stability when annealed in the presence of 50 mM KCl with T_{ms} of 86°C and 81°C, respectively (estimated as the temperature at which the molar ellipticity had been reduced by 50%), than those when annealed in 50 mM LiCl or no additional monovalent cation. Both mutant oligodeoxyribonucleotide YP-3M and oligoribonucleotide YU-4M exhibited decreased T_{ms} (53°C and 52°C, respectively, when annealed in the presence of 50 mM KCl) in comparison with the wild-type oligonucleotides, and reduced dependence of the melting curves on the local cationic environment (bottom panels of Figure 3C and D). These thermal stability data are consistent with the CD spectral results shown above in supporting the hypothesis that oligodeoxyribonucleotide YP-3 self-anneals in the presence of 50 mM KCl into a mixture of parallel and anti-parallel G4 DNA structures, and that oligoribonucleotide YU-4 self-anneals into a parallel G4 RNA structure.

In vitro footprinting of the YY1 promoter region with DNase I

DNase I preferentially cleaves locally unwound or normal duplex DNA regions versus single-stranded regions or secondary structures (72). When a supercoiled pGL3/YY1-short-prmt plasmid was incubated with 100 mM KCl and digested with DNase I, the primer extension reaction indicated a protected region approximately from −329 to −440 of the YY1 promoter, including the YP-3 sequence (−409 to −347), versus the condition without KCl addition (Figure 4, compare the two lanes at right). This result suggested a possible transition from B-DNA to a G-4 structure in the YY1 promoter region, which provided resistance to DNase I digestion, as previously demonstrated by Sun (60).

G4 structure-forming sequences present in the YY1 promoter and 5′-UTR modulate the expression of a reporter gene

As we observed the presence of the sequences with the potential of forming G4 structures in the promoter and 5′-UTR of YY1, we asked whether these structures may affect the expression of YY1. To answer this question, we first carried out reporter assays. As shown in Figure 5A, we generated five reporter constructs (see 'Materials and Methods' section for details). The constructs (a) and (b) employ the wild-type and the G4 structure-mutated YY1 promoters (−1703 to −1), respectively, to drive Gluc expression. The constructs (c) and (d) have the wild-type and the G4 structure-mutated YY1 5′-UTR sequences (+1 to +480) inserted between the PGK promoter and Gluc cDNA of an original reporter vector shown as (e) of Figure 5A. Reporter assays conducted in 293 T cells using the reporter plasmids (a) and (b) of the YY1

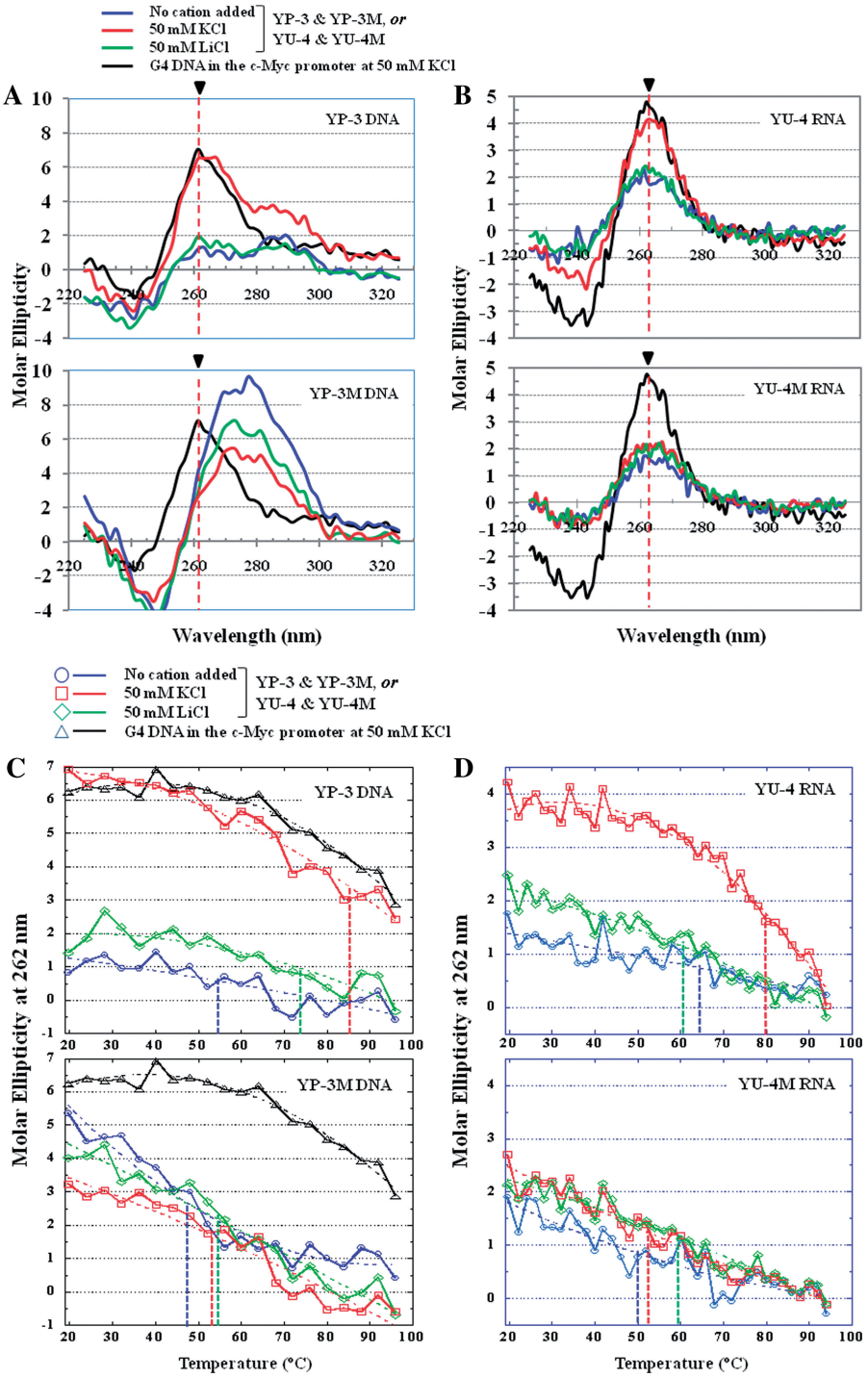

Figure 3. CD analyses of self-annealed oligodeoxyribonucleotide YP-3 or oligoribonucleotide YU-4 corresponding to sequences in the YY1 promoter and 5′-UTR, respectively. (**A** and **B**). Wavelength scan of (A) oligodeoxyribonucleotide YP-3 and (B) oligoribonucleotide YU-4 annealed in different monovalent cationic environments. (**C** and **D**). Thermal stability analyses of the secondary structure formed in self-annealed oligodeoxyribonucleotides or oligoribonucleotides corresponding to the sequences in the YY1 promoter and 5′-UTR, respectively. The molar ellipticity at 262 nm of the annealed oligonucleotides in different monovalent cationic environments was observed at different temperatures. The polynomial fitting curve of each raw data set is shown as a dished curve with the T_m indicated by a dropped dashed line in the same color.

promoter demonstrated that mutations of the nucleotides essential to G4 structure formation resulted in increased YY1 promoter activity (1.5-fold or 54% increase, $P = 0.01$, Figure 5B), suggesting an inhibitory role of the G4 motif in the YY1 promoter. The reporter assays using the plasmids (c) and (d) indicated that the mutation of the G4 structure in the YY1 5′-UTR could also promote the expression of the downstream Gluc (Figure 5C). We noticed that the empty vector (e) exhibited even higher expression than these two constructs

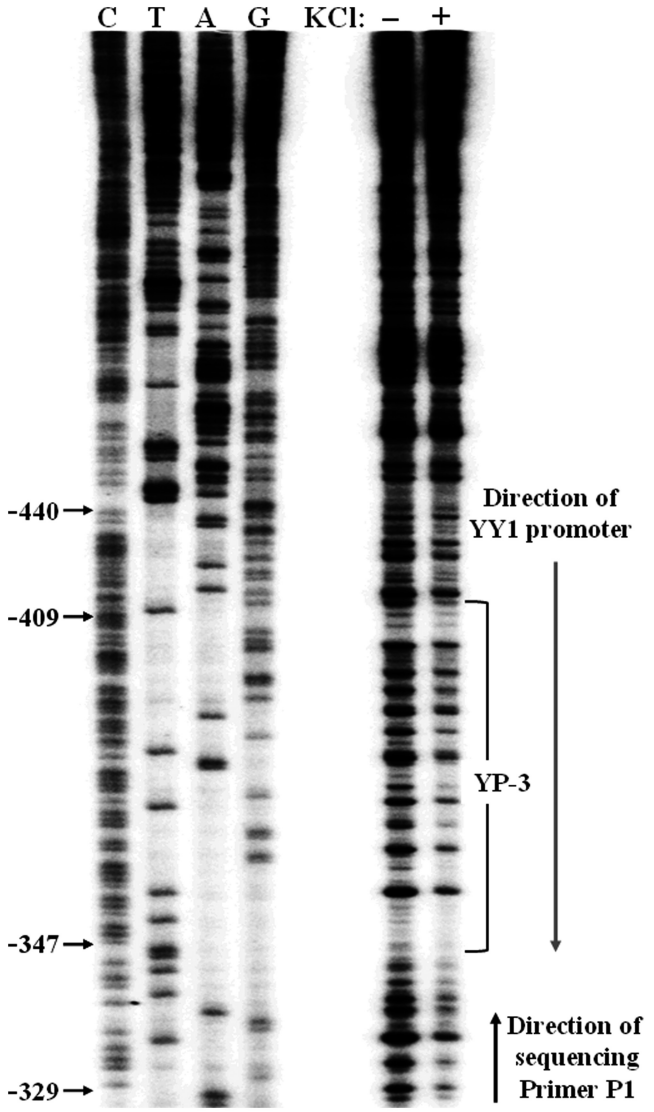

Figure 4. *In vitro* footprinting of the YY1 promoter region with DNase I. DNA sequencing and primer extension reactions were carried out as described in the 'Materials and Methods' section. The nucleotide numbers for the region resistant to DNase I digestion (−440 to −329) and the region of the YP-3 (−409 to −347) are marked on the left. The YP-3 region and the directions of the YY1 promoter and DNA sequencing are indicated on the right. The annotation (C,T,A,G) of DNA sequencing reaction for plasmid pGL3/YY1-short-prmt is according to the positive strand of the YY1 promoter. The primer extension of the same plasmid was conducted in the absence (−) and presence (+) of 100 mM KCl.

(c) and (d) containing the wild-type or mutated YY1 5′-UTR sequences, respectively. This could result from either the difference of the distance between the promoter and Gluc cDNA in these vectors, or the effects of other secondary structures in the inserted DNA fragments. Therefore, we normalized the Gluc activity of (c) and (d) by that of the vector alone (e) in Figure 5C. After this calculation, we observed that the G4 structure mutations in the YY1 5′-UTR led to a markedly increased expression of the downstream Gluc (2.4-fold or 142% increase, $P = 0.001$, Figure 5D).

The G4 nucleic acid resolvase G4R1 enhances reporter gene expression driven by the YY1 promoter but not the YY1 5′-UTR

Several helicases have been reported to resolve G4 structure (45,47). Among them, G4R1 possesses the capability of resolving both G4 DNA and G4 RNA motifs (50). To explore the mechanisms underlying the regulation of the G4 structures in the YY1 promoter and 5′-UTR, we carried out reporter assays to study the effects of G4R1 on these five reporter constructs described in Figure 5A. When G4R1 was cotransfected with the reporter plasmid (a), we detected an increased Gluc expression, compared to the sample transfected with an empty vector (1.5-fold or 45% increase, $P = 0.01$, columns 1 and 2 in Figure 6A). The YY1 promoter containing a mutated G4 sequence retained the response to ectopic G4R1 by an increased transcriptional activity (1.3-fold or 32% increase, $P = 0.003$, columns 3 and 4 in Figure 6A). This suggests that a concealed G4 motif(s) may exist in the YY1 promoter in addition to the one that we have identified.

We carried out experiments to test the effects of G4R1 on the YY1 5′-UTR-mediated expression. Both reporter constructs (c) and (d) containing the wild-type and G4 structure-mutated YY1 5′-UTR, respectively, could be stimulated by the transfected G4R1 (columns 5–8 in Figure 6B). However, the transcriptional activity of the PGK-Gluc vector without the YY1 5′-UTR insert could also be enhanced by the ectopic G4R1, indicating that the PGK promoter is also responsive to G4R1. We therefore normalized the data of columns 5–8 by the corresponding Gluc expression of the vector controls (columns 9 and 10). After this normalization, the relative expression of the reporter constructs with either wild-type or the G4 motif-mutated YY1 5′-UTR displayed very similar activity in the absence and presence of ectopic G4R1 (9.2% increase, $P = 0.49$, between columns 11 and 12; 4.2% decrease, $P = 0.33$, between columns 13 and 14; Figure 6C). These results indicate that the G4 sequence motif in the YY1 5′-UTR is unlikely a substrate of G4R1. It is noteworthy that the reporter construct with the mutated G4 structure still exhibited increased Gluc expression compared to the one with wild-type sequence (compare columns 13, 14 with 11, 12, Figure 6C), consistent with the observation in Figure 5D.

In vitro determination of the interaction and resolving activity of G4R1 on the YY1 G4 structures

As we have demonstrated the stimulatory effect of G4R1 on the YY1 promoter, we further studied the binding affinity of G4R1 to the G4 DNA sequence in the YY1 promoter *in vitro*. We carried out the electrophoretic mobility shift assay (EMSA) using recombinant G4R1 protein purified as previously described (55) and the ^{32}P-labeled oligodeoxyribonucleotide YP-3 or its mutated form YP-3M (Figure 2A). When ^{32}P-labeled YP-3 was incubated with increasing amounts of G4R1, slowly migrating bands with generally escalating intensity (compare lane 1 with lanes 2–6 in Figure 7A) were observed, which is likely the complex formed by the G4R1 and oligodeoxyribonucleotide YP-3. However,

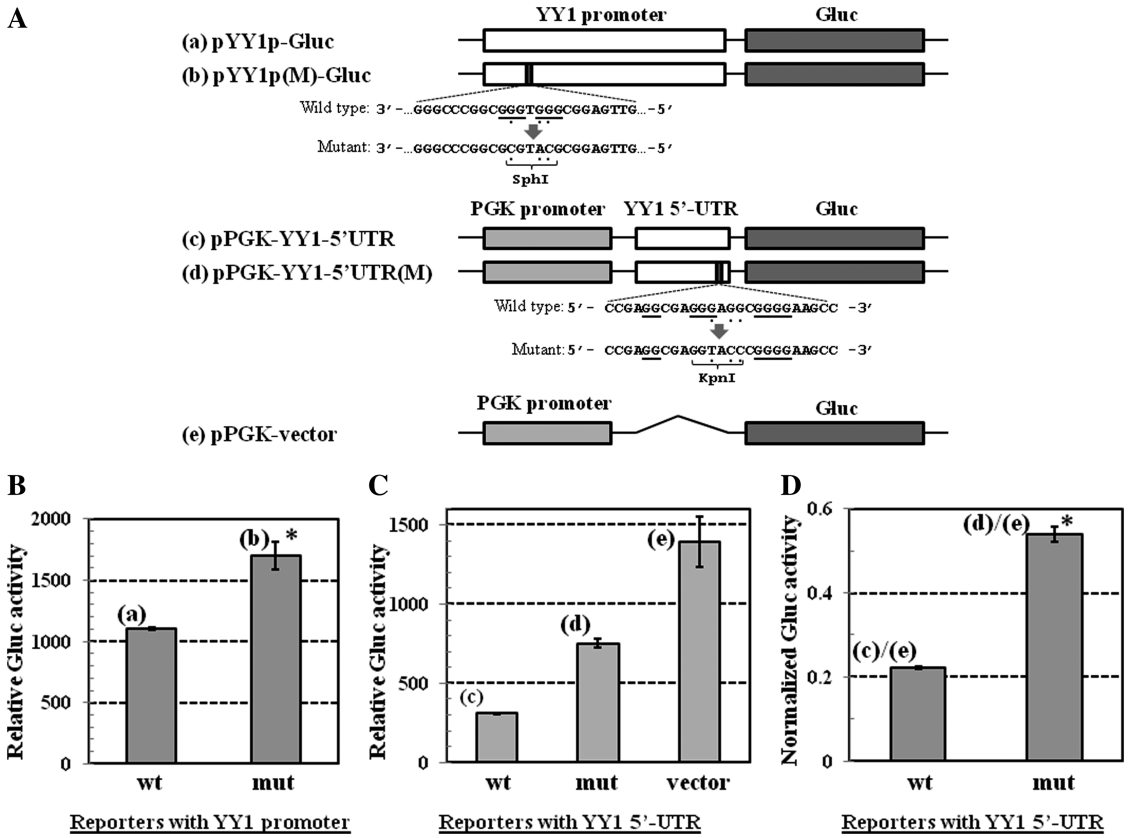

Figure 5. Reporter assay to study the effects of mutating potential G4 structure-forming sequences in the YY1 promoter and 5′-UTR on gene expression. (**A**) Schematic diagrams of the constructs generated for reporter assays. Constructs (a) and (b) employ the 1703 bp YY1 promoter to drive Gluc expression. Gluc expression in constructs (c), (d) and (e) was driven by the PGK promoter. Wild-type or mutated YY1 5′-UTR is inserted between the PGK promoter and Gluc cDNA in (c) and (d), respectively. The guanines with potential of forming G4 structures are underlined. The mutated guanines and the replacing bases are underneath labeled by dots. The introduced SphI and KpnI sites are indicated. Gluc, Gaussia luciferase; PGK, phosphoglycerate kinase. The mutated sites that altered the G4 structure-forming sequences are indicated as shadowed bars in the YY1 promoter and 5′-UTR. (**B** and **C**) Gluc activity of the reporter constructs containing the wild-type and mutated (B) YY1 promoter and (C) 5′-UTR sequences, respectively. (**D**) Normalized Gluc activity of the data in 'C'. Asterisk indicates significant changes.

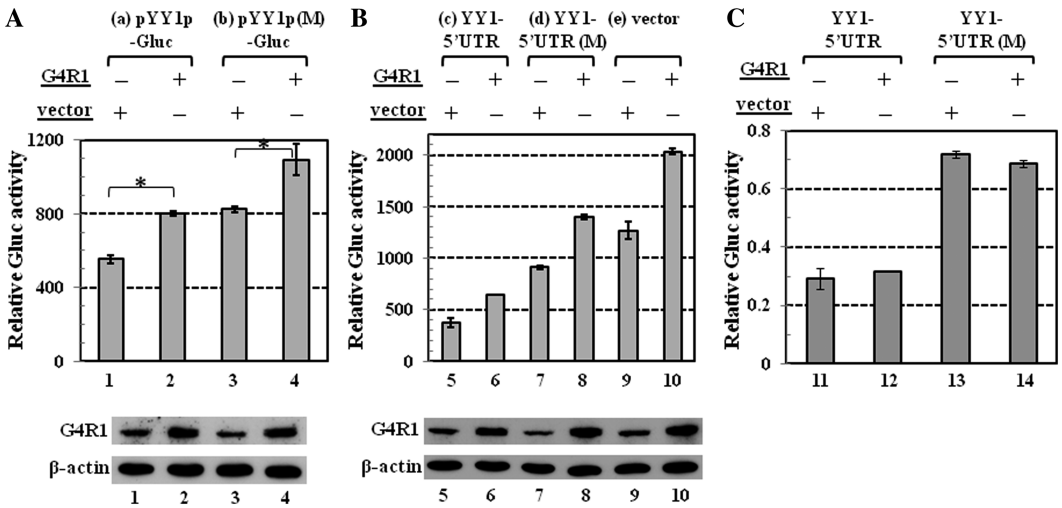

Figure 6. Effects of G4R1 on the expression mediated by the YY1 promoter and 5′-UTR. (**A** and **B**) Effects of G4R1 on Gluc expression mediated by (A) the YY1 promoter and (B) YY1 5′-UTR. In 'A', G4R1-expressing plasmid or the empty vector (500 ng) was cotransfected with either the reporter construct (a) containing wild-type YY1 promoter sequence, or (b) with mutated YY1 promoter sequence (200 ng, Figure 5A) in 24-well plate. In 'B', G4R1-expressing plasmid or the empty vector (500 ng) was individually cotransfected with the reporter constructs (c), (d) and (e) (200 ng). The ectopically expressed G4R1 with β-actin as loading controls was examined by western blots shown under the graphs. (**C**) Normalized Gluc activity of 'B'. Asterisk indicates significant changes.

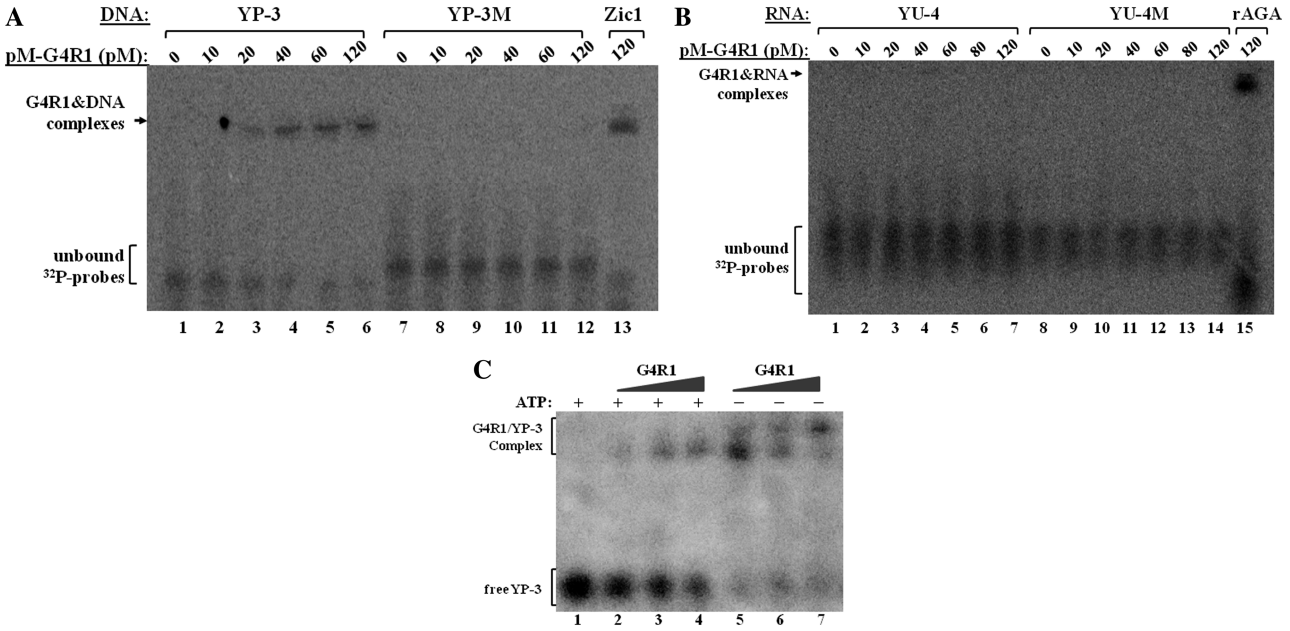

Figure 7. EMSA to study the interaction and resolvase activity of G4R1 to the YY1 G4 structures. (**A**) EMSA study to determine the interaction between G4R1 and oligodeoxyribonucleotide YP-3. An amount of 1 pM of 5′-^{32}P-labeled self-annealed YP-3 (lanes 1–6) and YP-3M (lanes 7–12) were incubated with increasing amounts of purified G4R1 (10–120 pM), as indicated on the top. An amount of 1 pM of 5′-^{32}P-labeled self-annealed PolyA Zic-1 oligodeoxyribonucleotide was used as a positive control. The position of G4R1–DNA complexes and the unbound 5′-^{32}P labeled oligodeoxyribonucleotides (or probes) are denoted on the left. (**B**) EMSA study to detect the interaction between G4R1 and oligoribonucleotide YU-4. Same as 'A', 5′-^{32}P-labeled self-annealed YU-4 (lanes 1–7) and YU-4M (lanes 8–14) were incubated with increasing amounts of purified G4R1 as indicated. An amount of 1 pM of 5′-^{32}P-labeled self-annealed rAGA was used as a positive control. (**C**) Gel mobility shift assay to detect ATP-dependency of G4R1/YP-3 association. An amount of 1 pM of 5′-^{32}P-labeled self-annealed YP-3 was incubated with increasing amounts (0, 25, 75 and 300 pM) of G4R1 in the presence and absence of 5 mM ATP. The samples were resolved by 10% non-denaturing polyacrylamide gel. The G4R1/YP-3 complexes and free YP-3 oligodeoxyribonucleotide are indicated.

YP-3M that contains mutated oligonucleotides in the G4 structure sequence failed to show any complex formation at the same conditions (lanes 7–12 in Figure 7A). In this study, we used a unimolecular G4 structure formed by self-annealing of an oligodeoxyribonucleotide whose sequence corresponds to the Zic-1 G4 DNA flanked by 10 adenines at each end (PolyA Zic-1 G4 DNA, see Figure 2A) (73) as a positive control (lane 13, Figure 7A), as we observed that PolyA Zic-1 G4 DNA efficiently associates with G4R1 (52). These results indicate that G4R1 can specifically bind to the G4 motif in the YY1 promoter. It is noteworthy that the free ^{32}P-labeled YP-3 migrated faster than the free ^{32}P-labeled YP-3 M, suggesting that the G4 motif made oligodeoxyribonucleotide YP-3 more compact and therefore faster migrating than the YP-3M with disrupted G4 structure.

We also assessed the binding affinity of G4R1 to the G4 structure of the oligoribonucleotide whose sequence is found in the YY1 5′-UTR. While the incubation of G4R1 with rAGA (Figure 2A), a G4-RNA that was previously demonstrated to associate with G4R1 (50), caused the appearance of a slowly migrated band (lane 15, Figure 7B), neither oligoribonucleotide YU-4 nor YU-4M showed any interaction with G4R1 (lanes 1–14).

To determine whether G4R1 resolves or stabilizes the G4 DNA structure in the YY1 promoter, we studied the G4R1 and YP-3 association in the presence and absence of ATP. In the presence of ATP, which is required for the resolvase activity of G4R1, we detected both G4R1/YP-3 complex and free YP-3 in comparison to the control with only annealed YP-3 (Figure 7C, lanes 2–4 versus lane 1). However, in the absence of ATP, the G4R1/YP-3 association was markedly increased, while the detected free YP-3 was largely reduced (lanes 5–7). This result suggests that G4R1 binds YP-3 tightly in the absence of ATP, but resolves and then releases YP-3 when ATP is provided. The binding, resolving and refolding are rapid and dynamic. Therefore, the free YP-3 could very quickly transform back to the favored compact G4 structures after being resolved by G4R1 and therefore the slowly migrated, unstructured YP-3 was not observed in the lanes 2–4 of Figure 7C.

G4R1 binds the YY1 promoter and its manipulated expression affects endogenous YY1 levels

As we observed the association of G4R1 and oligodeoxyribonucleotide YP-3 *in vitro*, we asked whether G4R1 binds the YY1 promoter in cells. Therefore, we carried out ChIP assays with the anti-G4R1 antibody, using non-specific IgG (sc-2343) as a negative control and histone H3 antibody as a positive control. As shown in the top panel of Figure 8A, G4R1 exhibited ~5-fold higher binding affinity than the control sample ($P = 0.004$), implicating that G4R1 directly regulates YY1 gene expression. As a positive control, the histone H3 antibody showed stronger signal than the G4R1

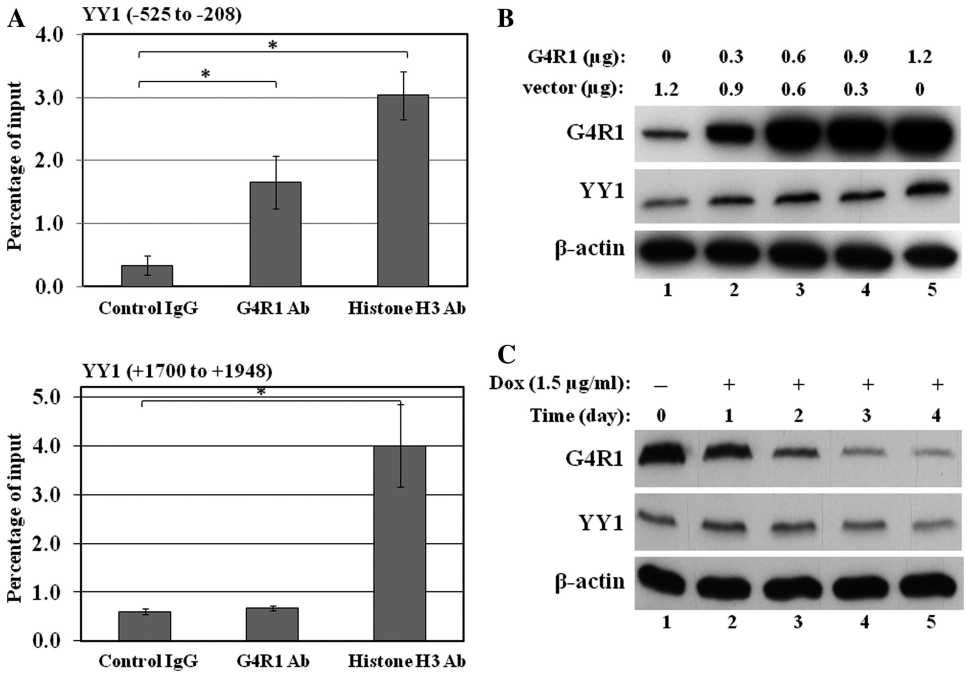

Figure 8. ChIP assay of G4R1 affinity to the YY1 promoter and effects of altered G4R1 expression on endogenous YY1 levels. (**A**) ChIP assay of the YY1 promoter. Non-specific mouse IgG (control), G4R1 antibody and histone H3 antibody were used in the immunoprecipitation. The amplified regions aligned to the YY1 promoter and mRNA (with transcription starting site designated as '+1') are indicated. The amounts of the YY1 DNA precipitated by these antibodies relative to the input are presented. The results are derived from three separate experiments. Asterisk indicates significant changes. (**B**) Effect of ectopic G4R1 on endogenous YY1 expression in 293 T cells. Increasing amounts of G4R1, as shown above the blot, were transfected into 293 T cells that expressing relatively low levels of endogenous G4R1. The cell lysates were analyzed by western blots using the antibodies indicated on the left. (**C**) Effects of G4R1 knockdown on endogenous YY1 expression in HeLa cells. HeLa cells that express high levels of endogenous G4R1 were infected by lentivirus expressing an inducible shRNA against G4R1 (54) cultured in medium containing 1.5 μg/ml of doxycycline (Dox) to induce the shRNA expression. The cells were collected at different time points as indicated on the top and the cell lysates were analyzed by western blots using the antibodies indicated on the left.

antibody. To exclude the non-specific binding of the G4R1 antibody, we also amplified a region in the YY1 exon 5 that has relatively low G/C content (17.3% of either G or C). As presented in the bottom panel of Figure 8A, only histone H3 antibody showed high binding affinity to this region, while G4R1 antibody exhibited comparable signal to the negative control antibody.

Since G4R1 binds to the YY1 promoter and stimulates its activity in driving Gluc expression in the reporter assays, we asked whether G4R1 affects the expression of endogenous YY1. We first transiently transfected increasing amounts of G4R1 into 293T cells, as they express relatively low levels of G4R1, and determined the endogenous YY1 levels by western blot. As shown in Figure 8B, YY1 expression was elevated with increasingly expressed G4R1. To determine whether G4R1 is required in maintaining endogenous YY1 expression, we inducibly knocked down G4R1 in HeLa cells that express high levels of G4R1. As shown in Figure 8C, the depletion of G4R1 only slightly reduced the levels of endogenous YY1, suggesting that G4R1 may not play a crucial role in maintaining YY1 expression.

G4R1 expression generally correlates with YY1 expression in breast cancer samples

As ectopic G4R1 affects endogenous YY1, we proceeded to determine whether there is any correlation between the expression levels of these two proteins. First, we took breast cancer as an example to test G4R1 and YY1 expression in some commonly used cell lines with normal human mammary epithelial cells (HMEC) as controls. We also included MCF-10A cells that are non-tumorigenic but immortalized. The tumorigenic cell lines included HEK (HMEC immortalized by SV40 large-T antigen, the telomerase catalytic subunit and an H-Ras) (74), SK-BR-3, ZR-75-1, BT-474 and MDA-MB-231. We analyzed an equal amount of cell lysates from these breast cell lines by western blot using antibodies for G4R1, YY1 (H-10) and β-actin. As shown in Figure 9A, non-tumorigenic MCF-10A cells and all tumor cell lines, except BT-474, expressed elevated G4R1 expression compared to HMEC, while YY1 levels are markedly increased in all tumor cell lines compared to MCF-10A and HMEC. These results suggest that both G4R1 and YY1 are overexpressed in most breast cancer cells. To determine whether G4R1 expression correlates with YY1 levels in primary human breast cancer, we analyzed a set of Affymetrix microarray expression profiles derived from the Uppsala breast cancer cohort consisting of 258 patient samples (64) using the probes indicated in the 'Materials and Methods' section. As shown in Figure 9B, the gene expression patterns of G4R1 and YY1 in these 258 breast tumors exhibited a significant correlation ($P = 4.5 \times 10^{-6}$, Pearson correlation), which is consistent with the results obtained from our *in vitro* studies.

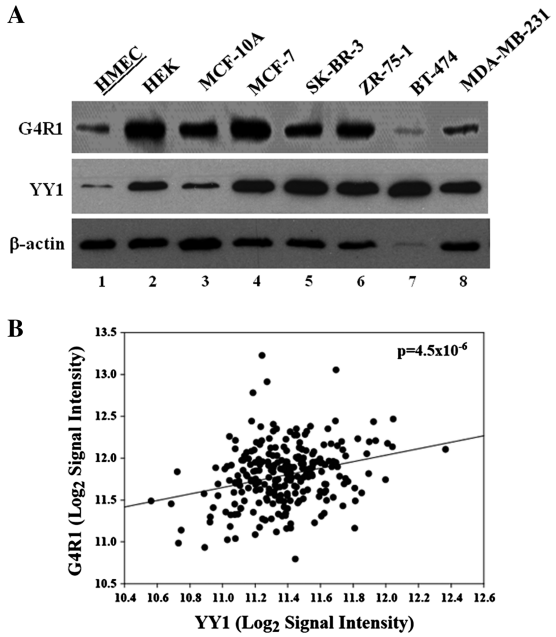

Figure 9. Studies of G4R1 and YY1 expression in breast cancer cell lines and patient samples. (**A**) G4R1 and YY1 expression in different non-malignant and malignant breast cell lines. Total cell lysates of the cell lines (labeled on the top) were analyzed by western blot (antibodies labeled on the left). HMEC and MCF-10A were used as non-malignant controls. HEK cells are a breast cancer cell line immortalized by SV40 large-T antigen (74). (**B**) Analysis of the expression correlation between G4R1 and YY1 in breast cancer samples in the Uppsala breast cancer cohort consisting of 258 patient samples. The signal intensities of G4R1 and YY1 were logarithmically transformed. A significant, positive correlation is suggested by the Pearson Product Moment Correlation *P*-value of 4.5×10^6.

DISCUSSION

The regulatory activities of YY1 in different epigenetic processes have implicated its critical role in cell proliferation, differentiation and tumorigenesis. As a multifunctional transcription factor, YY1 has been extensively studied in its regulation towards the expression of various target genes. However, the mechanisms underlying how YY1 gene expression is regulated are relatively understudied. In this report, we revealed the G/C rich features in the vicinity of the YY1 transcription start site on the human YY1 promoter and 5′-UTR. We then provided clear *in vitro* evidence to demonstrate that these regions contain sequences capable of forming G4 DNA and RNA structures, respectively, and that mutations of these G4 structure-forming sequences affected the YY1 promoter-mediated Gluc expression or that downstream of the YY1 5′-UTR in reporter assays. Our mechanistic studies also suggested that the G4 nucleic acid resolvase G4R1 may release the G4 structure in the YY1 promoter, but not the one in the YY1 5′-UTR. To investigate the biological relevance of our study, we also analyzed the gene array of 258 human breast cancer samples and discovered the significant correlation between G4R1 and YY1 gene expression.

In the promoter region, G4 DNA structures that regulate the gene expression may exist in either the positive or negative strand. It is noteworthy that cytosine rich (C-rich) DNA sequences may form i-motifs that have been indicated to regulate the expression of multiple genes, including Bcl-2 and c-Myc (75,76). Therefore, it is reasonable to predict that, while G4 motifs are present in one strand, structures such as i-motifs can also be formed in the Watson–Crick complementary strand. They may collaboratively regulate the transcriptional activity of the YY1 promoter, as described in a model for the c-Myc promoter (40).

The YY1 promoter likely forms multiple G4 structures due to its high G/C content and it is not practical for us to determine all of them in this study. However, our results strongly indicated the presence and regulatory role of the G4 structure in the YY1 promoter. In the YP-3 oligonucleotide, there are 7–9 isolated G-runs ($\geq$3 Gs) and our stoichiometry experiment suggested the majority of this oligonucleotide formed intramolecular structures. Therefore, we predict that the YP-3 oligonucleotide forms multiple, dynamic G4 structures among these G-runs that may rapidly interchange, leading to the protection of multiple guanines in the DMS footprinting assay (Figure 2C). Consistently, our CD studies also suggested the presence of G4 structures with anti-parallel strands in the YP-3 (Figure 2B). The dynamic G4 structure formation has been demonstrated previously (77,78), which makes it technically challenging to create a schematic picture to present the predicted G4 structures and would be beyond the scope of this current study.

We demonstrated an interaction of G4R1 with the G4 sequence motif in the YY1 promoter, as well as a stimulatory effect of G4R1 on the expression driven by the YY1 promoter. However, we also observed that G4R1 could still enhance the expression of the reporter construct driven by the G4 structure-mutated YY1 promoter, as shown in Figure 6A. Since the region close to the transcription start site in the YY1 promoter is highly G/C rich, this effect could result from other G4 DNA structure(s) that has not been identified. It is also possible that the activity of the YY1 promoter is inhibited by other types of structures, which can be resolved by G4R1.

In the EMSA studies, we did not detect large amounts of unbound oligonucleotides (Figure 7), since only 1 pM of 5′-^{32}P-labeled self-annealed YP-3 oligonucleotide was incubated with 10–300 pM of G4R1. The reason to use this ratio is that these concentrations represent standard binding affinity determination conditions. When determining the binding affinity of an annealed oligonucleotide, it is important that the oligonucleotide is used at a much lower concentration than that of the resolvase. Given the extraordinarily tight binding affinity of G4R1 for G4 nucleic acids (52), the concentration of the G4 oligonucleotides should be kept close to 1 pM. As shown in Figure 7C, G4R1 tightly bound YP-3 in the absence of ATP. This binding interaction at low YP-3 concentrations is strongly indicative of the presence of G4 structures in YP-3, as G4R1 prefers to bind G4 nucleic acids in comparison to unstructured single stranded DNA or Watson-Crick duplex DNA by at least 3 orders of magnitude (50,55). YP-3 was released from the G4R1 after resolution of the G4 structure when ATP was added (52). This result strongly suggests

that G4R1 resolves the G4 structure in the YP-3 oligonucleotide.

When testing the effects of the YY1 5′-UTR on the expression of downstream Gluc, we employed the PGK promoter. In our study, we observed that this promoter can be stimulated by G4R1, suggesting that it may contain G4 DNA structure motif(s). It is certainly possible that G4R1 possesses other activities, in addition to resolving G4 structures, which may generally promote gene expression. After examining the DNA sequence, we found that this promoter is indeed G/C rich (>63%) and has multiple G- or C-runs. We also checked several other commonly used promoters with medium expression strengths, including chicken β-actin and ubiquitin C promoters. They both have high G/C contents and potential G4 DNA-forming sequences. CMV promoter has nearly equal amounts between G/C and A/T, but its robust expression strength could overwhelm the effect of G4R1 on any putative G4 structure. Therefore, we still used the PGK promoter to study the YY1 5′-UTR-mediated expression and compensated the effects of G4R1 by normalizing the data against those of the reporter construct without the YY1 5′-UTR insert. After this data processing, we concluded that the YY1 5′-UTR-mediated Gluc expression was unresponsive to the ectopically introduced G4R1. Consistently, G4R1 did not bind to oligoribonucleotide YU-4 in our EMSA study (Figure 7B). Whether the G4 RNA motif in the YY1 5′-UTR is a substrate of other resolvases, such as BLM, WRN, or FANCJ, needs further investigation. It is likely that multiple G4 structures may exist in the 480-nt YY1 5′-UTR with such a high G content (44.4%), a speculation that is supported by the CD studies of the oligonucleotides YU-1 and YU-2 (Figure 2B). However, we believe that G4R1 does not bind these two oligonucleotides, since the expression of the reporter construct containing the entire 5′-UTR region of YY1 was not affected by ectopic G4R1.

While G4R1 may possess general stimulatory effects on gene expression, especially oncogenes that have G4 structures in their promoters, our data from the CD spectral study, reporter assay and correlated G4R1-YY1 gene expression strongly suggest that YY1 is one of G4R1 target genes and this regulation may contribute to cancer development. It is noteworthy that G4R1 knockdown did not markedly affect endogenous YY1 levels, although ectopically expressed G4R1 led to an increased YY1 expression (Figure 8B and C). This indicates that YY1 expression is modulated by multiple regulatory mechanisms, in addition to G4 DNA/G4R1. Based on our data, G4R1 likely plays a role in promoting, but not maintaining, YY1 expression.

The sequences of the G4 structures may contain or overlap with the binding sites of certain transcription factors. Thus, it is possible that the mutagenesis of the guanines essential to G4 structure formation in the YY1 promoter could alter the affinity of certain transcription factor(s), likely repressor(s), and in turn enhance the promoter activity in reporter assays. This dilemma is a generic issue in the field of G4 structure research. In our studies, in addition to the data from reporter assays that demonstrated the effects of G4 DNA-forming sequence and G4R1 on the YY1 promoter-mediated gene expression, we also presented spectroscopic evidence from CD analyses and protection of the YY1 G4 DNA structure from DMS-mediated methylation and DNase I digestion. All data sets support the presence and the regulatory role of G4 structure in the YY1 promoter.

Numerous reports demonstrated the potential regulation of YY1 in tumorigenesis. Although most studies suggest an oncogenic or proliferative role of YY1 in cancer development and progression [see the review (3)], a handful reports also proposed the possible anti-cancer activities of YY1 (10,79–81). Statistical analysis indicates that G4 structures are present in the promoters of most proto-oncogenes, while the promoters of tumor suppressors have very low levels of guanine runs (43). Therefore, our current study showing the G/C rich feature and the presence of quadruplex in the YY1 promoter supports the theory of YY1 as an oncogene.

SUPPLEMENTARY DATA

Supplementary Data are available at NAR Online: Supplementary Figures S1–S3.

ACKNOWLEDGEMENTS

The authors thank Drs Yuh-Hwa Wang, Daekyu Sun, Steven Smith, Zhiyong Deng and Mr Jason Fye for helpful discussions, and Eric D. Routh for technical supports. The authors acknowledge Drs Fred W. Perrino, Greg Kucera and Suzy V. Torti for the accesses of their equipments, and the Cell and Virus Vector Core Laboratory of the Comprehensive Cancer Center at WFUHS for the provision of cell culture materials.

FUNDING

American Cancer Society (RSG-09-082-01-MGO); Department of Cancer Biology and Comprehensive Cancer Center of Wake Forest University startup fund to G.S.; China Scholarship Council (CSC) Program (to W.H.); National Cancer Institute training (Grant 5T32CA079448-09 to P.J.S., P.C. and B.G.); Program for New Century Excellent Talents in University (NCET-08-0467 to M.L.). Funding for open access charge: American Cancer Society (RSG-09-082-01-MGO); Department of Cancer Biology and Comprehensive Cancer Center of Wake Forest University startup fund (to G.S.); CSC Program; Program for New Century Excellent Talents in University (NCET-08-0467).

Conflict of interest statement. None declared.

REFERENCES

1. Shi,Y., Seto,E., Chang,L.S. and Shenk,T. (1991) Transcriptional repression by YY1, a human GLI-Kruppel-related protein, and relief of repression by adenovirus E1A protein. *Cell*, **67**, 377–388.
2. Shi,Y., Lee,J.S. and Galvin,K.M. (1997) Everything you have ever wanted to know about Yin Yang 1.... *Biochim. Biophys. Acta*, **1332**, F49–F66.

3. Sui,G. (2009) The regulation of YY1 in tumorigenesis and its targeting potential in cancer therapy. *Mol. Cell. Pharmacol.*, **1**, 157–176.
4. Thomas,M.J. and Seto,E. (1999) Unlocking the mechanisms of transcription factor YY1: are chromatin modifying enzymes the key? *Gene*, **236**, 197–208.
5. Gordon,S., Akopyan,G., Garban,H. and Bonavida,B. (2006) Transcription factor YY1: structure, function, and therapeutic implications in cancer biology. *Oncogene*, **25**, 1125–1142.
6. Atchison,L., Ghias,A., Wilkinson,F., Bonini,N. and Atchison,M.L. (2003) Transcription factor YY1 functions as a PcG protein in vivo. *EMBO J.*, **22**, 1347–1358.
7. Lee,T.C., Zhang,Y. and Schwartz,R.J. (1994) Bifunctional transcriptional properties of YY1 in regulating muscle actin and c-myc gene expression during myogenesis. *Oncogene*, **9**, 1047–1052.
8. Zhou,Q., Gedrich,R.W. and Engel,D.A. (1995) Transcriptional repression of the c-fos gene by YY1 is mediated by a direct interaction with ATF/CREB. *J. Virol.*, **69**, 4323–4330.
9. Begon,D.Y., Delacroix,L., Vernimmen,D., Jackers,P. and Winkler,R. (2005) Yin Yang 1 cooperates with activator protein 2 to stimulate ERBB2 gene expression in mammary cancer cells. *J. Biol. Chem.*, **280**, 24428–24434.
10. Furlong,E.E., Rein,T. and Martin,F. (1996) YY1 and NF1 both activate the human p53 promoter by alternatively binding to a composite element, and YY1 and E1A cooperate to amplify p53 promoter activity. *Mol. Cell Biol.*, **16**, 5933–5945.
11. Delehouzee,S., Yoshikawa,T., Sawa,C., Sawada,J., Ito,T., Omori,M., Wada,T., Yamaguchi,Y., Kabe,Y. and Handa,H. (2005) GABP, HCF-1 and YY1 are involved in Rb gene expression during myogenesis. *Genes Cells*, **10**, 717–731.
12. Schlisio,S., Halperin,T., Vidal,M. and Nevins,J.R. (2002) Interaction of YY1 with E2Fs, mediated by RYBP, provides a mechanism for specificity of E2F function. *EMBO J.*, **21**, 5775–5786.
13. Wu,F. and Lee,A.S. (2001) YY1 as a regulator of replication-dependent hamster histone H3.2 promoter and an interactive partner of AP-2. *J. Biol. Chem.*, **276**, 28–34.
14. Last,T.J., van Wijnen,A.J., Birnbaum,M.J., Stein,G.S. and Stein,J.L. (1999) Multiple interactions of the transcription factor YY1 with human histone H4 gene regulatory elements. *J. Cell. Biochem.*, **72**, 507–516.
15. Yakovleva,T., Kolesnikova,L., Vukojevic,V., Gileva,I., Tan-No,K., Austen,M., Luscher,B., Ekstrom,T.J., Terenius,L. and Bakalkin,G. (2004) YY1 binding to a subset of p53 DNA-target sites regulates p53-dependent transcription. *Biochem. Biophys. Res. Commun.*, **318**, 615–624.
16. Lee,J.S., Galvin,K.M., See,R.H., Eckner,R., Livingston,D., Moran,E. and Shi,Y. (1995) Relief of YY1 transcriptional repression by adenovirus E1A is mediated by E1A-associated protein p300. *Genes Dev.*, **9**, 1188–1198.
17. Yang,W.M., Inouye,C., Zeng,Y., Bearss,D. and Seto,E. (1996) Transcriptional repression by YY1 is mediated by interaction with a mammalian homolog of the yeast global regulator RPD3. *Proc. Natl Acad. Sci. USA*, **93**, 12845–12850.
18. Yao,Y.L., Yang,W.M. and Seto,E. (2001) Regulation of transcription factor YY1 by acetylation and deacetylation. *Mol. Cell Biol.*, **21**, 5979–5991.
19. Wang,L., Brown,J.L., Cao,R., Zhang,Y., Kassis,J.A. and Jones,R.S. (2004) Hierarchical recruitment of polycomb group silencing complexes. *Mol. Cell.*, **14**, 637–646.
20. Caretti,G., Di Padova,M., Micales,B., Lyons,G.E. and Sartorelli,V. (2004) The Polycomb Ezh2 methyltransferase regulates muscle gene expression and skeletal muscle differentiation. *Genes Dev.*, **18**, 2627–2638.
21. Rezai-Zadeh,N., Zhang,X., Namour,F., Fejer,G., Wen,Y.D., Yao,Y.L., Gyory,I., Wright,K. and Seto,E. (2003) Targeted recruitment of a histone H4-specific methyltransferase by the transcription factor YY1. *Genes Dev.*, **17**, 1019–1029.
22. Sui,G., Affar el,B., Shi,Y., Brignone,C., Wall,N.R., Yin,P., Donohoe,M., Luke,M.P., Calvo,D., Grossman,S.R. *et al.* (2004) Yin Yang 1 is a negative regulator of p53. *Cell*, **117**, 859–872.
23. Petkova,V., Romanowski,M.J., Sulijoadikusumo,I., Rohne,D., Kang,P., Shenk,T. and Usheva,A. (2001) Interaction between YY1 and the retinoblastoma protein. Regulation of cell cycle progression in differentiated cells. *J. Biol. Chem.*, **276**, 7932–7936.
24. Cunningham,J.T., Rodgers,J.T., Arlow,D.H., Vazquez,F., Mootha,V.K. and Puigserver,P. (2007) mTOR controls mitochondrial oxidative function through a YY1-PGC-1alpha transcriptional complex. *Nature*, **450**, 736–740.
25. Weis,L. and Reinberg,D. (1997) Accurate positioning of RNA polymerase II on a natural TATA-less promoter is independent of TATA-binding-protein-associated factors and initiator-binding proteins. *Mol. Cell Biol.*, **17**, 2973–2984.
26. Kuzmichev,A., Jenuwein,T., Tempst,P. and Reinberg,D. (2004) Different EZH2-containing complexes target methylation of histone H1 or nucleosomal histone H3. *Mol. Cell.*, **14**, 183–193.
27. Gronroos,E., Terentiev,A.A., Punga,T. and Ericsson,J. (2004) YY1 inhibits the activation of the p53 tumor suppressor in response to genotoxic stress. *Proc. Natl Acad. Sci. USA*, **101**, 12165–12170.
28. Bain,M. and Sinclair,J. (2005) Targeted inhibition of the transcription factor YY1 in an embryonal carcinoma cell line results in retarded cell growth, elevated levels of p53 but no increase in apoptotic cell death. *Eur. J. Cell Biol.*, **84**, 543–553.
29. Santiago,F.S., Ishii,H., Shafi,S., Khurana,R., Kanellakis,P., Bhindi,R., Ramirez,M.J., Bobik,A., Martin,J.F., Chesterman,C.N. *et al.* (2007) Yin Yang-1 inhibits vascular smooth muscle cell growth and intimal thickening by repressing p21WAF1/Cip1 transcription and p21WAF1/Cip1-Cdk4-cyclin D1 assembly. *Circ. Res.*, **101**, 146–155.
30. Gu,W. and Roeder,R.G. (1997) Activation of p53 sequence-specific DNA binding by acetylation of the p53 C-terminal domain. *Cell*, **90**, 595–606.
31. Luo,J., Su,F., Chen,D., Shiloh,A. and Gu,W. (2000) Deacetylation of p53 modulates its effect on cell growth and apoptosis. *Nature*, **408**, 377–381.
32. Barlev,N.A., Liu,L., Chehab,N.H., Mansfield,K., Harris,K.G., Halazonetis,T.D. and Berger,S.L. (2001) Acetylation of p53 activates transcription through recruitment of coactivators/histone acetyltransferases. *Mol. Cell.*, **8**, 1243–1254.
33. Li,M., Luo,J., Brooks,C.L. and Gu,W. (2002) Acetylation of p53 inhibits its ubiquitination by Mdm2. *J. Biol. Chem.*, **277**, 50607–50611.
34. Seligson,D., Horvath,S., Huerta-Yepez,S., Hanna,S., Garban,H., Roberts,A., Shi,T., Liu,X., Chia,D., Goodglick,L. *et al.* (2005) Expression of transcription factor Yin Yang 1 in prostate cancer. *Int. J. Oncol.*, **27**, 131–141.
35. Erkeland,S.J., Valkhof,M., Heijmans-Antonissen,C., Delwel,R., Valk,P.J., Hermans,M.H. and Touw,I.P. (2003) The gene encoding the transcriptional regulator Yin Yang 1 (YY1) is a myeloid transforming gene interfering with neutrophilic differentiation. *Blood*, **101**, 1111–1117.
36. de Nigris,F., Botti,C., de Chiara,A., Rossiello,R., Apice,G., Fazioli,F., Fiorito,C., Sica,V. and Napoli,C. (2006) Expression of transcription factor Yin Yang 1 in human osteosarcomas. *Eur. J. Cancer*, **42**, 2420–2424.
37. de Nigris,F., Botti,C., Rossiello,R., Crimi,E., Sica,V. and Napoli,C. (2007) Cooperation between Myc and YY1 provides novel silencing transcriptional targets of alpha3beta1-integrin in tumour cells. *Oncogene*, **26**, 382–394.
38. Baritaki,S., Sifakis,S., Huerta-Yepez,S., Neonakis,I.K., Soufla,G., Bonavida,B. and Spandidos,D.A. (2007) Overexpression of VEGF and TGF-beta1 mRNA in Pap smears correlates with progression of cervical intraepithelial neoplasia to cancer: implication of YY1 in cervical tumorigenesis and HPV infection. *Int. J. Oncol.*, **31**, 69–79.
39. Kim,J.D., Yu,S. and Kim,J. (2009) YY1 is autoregulated through its own DNA-binding sites. *BMC Mol. Biol.*, **10**, 85.
40. Brooks,T.A., Kendrick,S. and Hurley,L. (2010) Making sense of G-quadruplex and i-motif functions in oncogene promoters. *FEBS J.*, **277**, 3459–3469.
41. Huppert,J.L. and Balasubramanian,S. (2007) G-quadruplexes in promoters throughout the human genome. *Nucleic Acids Res.*, **35**, 406–413.
42. Phan,A.T. Human telomeric G-quadruplex: structures of DNA and RNA sequences. *FEBS J.*, **277**, 1107–1117.
43. Eddy,J. and Maizels,N. (2006) Gene function correlates with potential for G4 DNA formation in the human genome. *Nucleic Acids Res.*, **34**, 3887–3896.

44. Hanahan,D. and Weinberg,R.A. (2000) The hallmarks of cancer. *Cell*, **100**, 57–70.
45. Wu,Y. and Brosh,R.M. Jr (2010) Helicase-inactivating mutations as a basis for dominant negative phenotypes. *Cell Cycle*, **9**, 4080–4090.
46. Chakraborty,P. and Grosse,F. (2011) Human DHX9 helicase preferentially unwinds RNA-containing displacement loops (R-loops) and G-quadruplexes. *DNA Repair*, **10**, 654–665.
47. Baran,N., Pucshansky,L., Marco,Y., Benjamin,S. and Manor,H. (1997) The SV40 large T-antigen helicase can unwind four stranded DNA structures linked by G-quartets. *Nucleic Acids Res.*, **25**, 297–303.
48. Sun,H., Karow,J.K., Hickson,I.D. and Maizels,N. (1998) The Bloom's syndrome helicase unwinds G4 DNA. *J. Biol. Chem.*, **273**, 27587–27592.
49. Wu,Y., Shin-ya,K. and Brosh,R.M. Jr (2008) FANCJ helicase defective in Fanconia anemia and breast cancer unwinds G-quadruplex DNA to defend genomic stability. *Mol. Cell. Biol.*, **28**, 4116–4128.
50. Creacy,S.D., Routh,E.D., Iwamoto,F., Nagamine,Y., Akman,S.A. and Vaughn,J.P. (2008) G4 resolvase 1 binds both DNA and RNA tetramolecular quadruplex with high affinity and is the major source of tetramolecular quadruplex G4-DNA and G4-RNA resolving activity in HeLa cell lysates. *J. Biol. Chem.*, **283**, 34626–34634.
51. Harrington,C., Lan,Y. and Akman,S.A. (1997) The identification and characterization of a G4-DNA resolvase activity. *J. Biol. Chem.*, **272**, 24631–24636.
52. Giri,B., Smaldino,P.J., Thys,R.G., Creacy,S.D., Routh,E.D., Hantgan,R.R., Lattmann,S., Nagamine,Y., Akman,S.A. and Vaughn,J.P. (2011) G4 Resolvase 1 tightly binds and unwinds unimolecular G4-DNA. *Nucleic Acids Res.*, **39**, 7161–7178.
53. Safrany,G. and Perry,R.P. (1993) Characterization of the mouse gene that encodes the delta/YY1/NF-E1/UCRBP transcription factor. *Proc. Natl Acad. Sci. USA*, **90**, 5559–5563.
54. Iwamoto,F., Stadler,M., Chalupnikova,K., Oakeley,E. and Nagamine,Y. (2008) Transcription-dependent nucleolar cap localization and possible nuclear function of DExH RNA helicase RHAU. *Exp. Cell Res.*, **314**, 1378–1391.
55. Vaughn,J.P., Creacy,S.D., Routh,E.D., Joyner-Butt,C., Jenkins,G.S., Pauli,S., Nagamine,Y. and Akman,S.A. (2005) The DEXH protein product of the DHX36 gene is the major source of tetramolecular quadruplex G4-DNA resolving activity in HeLa cell lysates. *J. Biol. Chem.*, **280**, 38117–38120.
56. Sun,D. and Hurley,L.H. (2010) Biochemical techniques for the characterization of G-quadruplex structures: EMSA, DMS footprinting, and DNA polymerase stop assay. *Methods Mol. Biol.*, **608**, 65–79.
57. Cogoi,S. and Xodo,L.E. (2006) G-quadruplex formation within the promoter of the KRAS proto-oncogene and its effect on transcription. *Nucleic Acids Res.*, **34**, 2536–2549.
58. Pichersky,E. (2000) DNA sequencing by the chemical method. In Rapley,R. (ed.), *The Nucleic Acid Protocols Handbook*. Humana Press Inc., Totowa, NJ, pp. 553–556.
59. Sun,D. and Hurley,L.H. (2009) The importance of negative superhelicity in inducing the formation of G-quadruplex and i-motif structures in the c-Myc promoter: implications for drug targeting and control of gene expression. *J. Med. Chem.*, **52**, 2863–2874.
60. Sun,D. (2010) In vitro footprinting of promoter regions within supercoiled plasmid DNA. *Methods Mol. Biol.*, **613**, 223–233.
61. Lattmann,S., Stadler,M.B., Vaughn,J.P., Akman,S.A. and Nagamine,Y. (2011) The DEAH-box RNA helicase RHAU binds an intramolecular RNA G-quadruplex in TERC and associates with telomerase holoenzyme. *Nucleic Acids Res.*, August 16 (doi:10.1093/nar/gkr630; epub ahead of print).
62. Deng,Z., Wan,M., Cao,P., Rao,A., Cramer,S.D. and Sui,G. (2009) Yin Yang 1 regulates the transcriptional activity of androgen receptor. *Oncogene*, **28**, 3746–3757.
63. Wan,C., Kulkarni,A. and Wang,Y.H. (2010) ATR preferentially interacts with common fragile site FRA3B and the binding requires its kinase activity in response to aphidicolin treatment. *Mutat. Res.*, **686**, 39–46.
64. Miller,L.D., Smeds,J., George,J., Vega,V.B., Vergara,L., Ploner,A., Pawitan,Y., Hall,P., Klaar,S., Liu,E.T. *et al.* (2005) An expression signature for p53 status in human breast cancer predicts mutation status, transcriptional effects, and patient survival. *Proc. Natl Acad. Sci. USA*, **102**, 13550–13555.
65. Yao,Y.L., Dupont,B.R., Ghosh,S., Fang,Y., Leach,R.J. and Seto,E. (1998) Cloning, chromosomal localization and promoter analysis of the human transcription factor YY1. *Nucleic Acids Res.*, **26**, 3776–3783.
66. Huppert,J.L. and Balasubramanian,S. (2005) Prevalence of quadruplexes in the human genome. *Nucleic Acids Res.*, **33**, 2908–2916.
67. Seenisamy,J., Rezler,E.M., Powell,T.J., Tye,D., Gokhale,V., Joshi,C.S., Siddiqui-Jain,A. and Hurley,L.H. (2004) The dynamic character of the G-quadruplex element in the c-MYC promoter and modification by TMPyP4. *J. Am. Chem. Soc.*, **126**, 8702–8709.
68. Lee,J.Y., Yoon,J., Kihm,H.W. and Kim,D.S. (2008) Structural diversity and extreme stability of unimolecular Oxytricha nova telomeric G-quadruplex. *Biochemistry*, **47**, 3389–3396.
69. Nambiar,M., Goldsmith,G., Moorthy,B.T., Lieber,M.R., Joshi,M.V., Choudhary,B., Hosur,R.V. and Raghavan,S.C. (2010) Formation of a G-quadruplex at the BCL2 major breakpoint region of the t(14;18) translocation in follicular lymphoma. *Nucleic Acids Res.*, 10.1093/nar/gkq1824.
70. Mergny,J.L., De Cian,A., Ghelab,A., Sacca,B. and Lacroix,L. (2005) Kinetics of tetramolecular quadruplexes. *Nucleic Acids Res.*, **33**, 81–94.
71. Liu,H., Kugimiya,A., Sakurai,T., Katahira,M. and Uesugi,S. (2002) A comparison of the properties and the solution structure for RNA and DNA quadruplexes which contain two GGAGG sequences joined with a tetranucleotide linker. *Nucleosides Nucleotides Nucleic Acids*, **21**, 785–801.
72. Saluz,H.P. and Jost,J.P. (1993) Approaches to characterize protein-DNA interactions in vivo. *Crit. Rev. Eukaryot Gene Expr.*, **3**, 1–29.
73. Arora,A., Dutkiewicz,M., Scaria,V., Hariharan,M., Maiti,S. and Kurreck,J. (2008) Inhibition of translation in living eukaryotic cells by an RNA G-quadruplex motif. *RNA*, **14**, 1290–1296.
74. Elenbaas,B., Spirio,L., Koerner,F., Fleming,M.D., Zimonjic,D.B., Donaher,J.L., Popescu,N.C., Hahn,W.C. and Weinberg,R.A. (2001) Human breast cancer cells generated by oncogenic transformation of primary mammary epithelial cells. *Genes Dev.*, **15**, 50–65.
75. Kendrick,S., Akiyama,Y., Hecht,S.M. and Hurley,L.H. (2009) The i-motif in the bcl-2 P1 promoter forms an unexpectedly stable structure with a unique 8:5:7 loop folding pattern. *J. Am. Chem. Soc.*, **131**, 17667–17676.
76. Dexheimer,T.S., Carey,S.S., Zuohe,S., Gokhale,V.M., Hu,X., Murata,L.B., Maes,E.M., Weichsel,A., Sun,D., Meuillet,E.J. *et al.* (2009) NM23-H2 may play an indirect role in transcriptional activation of c-myc gene expression but does not cleave the nuclease hypersensitive element III1. *Mol. Cancer Ther.*, **8**, 1363–1377.
77. Dailey,M.M., Miller,M.C., Bates,P.J., Lane,A.N. and Trent,J.O. (2010) Resolution and characterization of the structural polymorphism of a single quadruplex-forming sequence. *Nucleic Acids Res.*, **38**, 4877–4888.
78. Miller,M.C. and Trent,J.O. (2011) Resolution of quadruplex polymorphism by size-exclusion chromatography. In Serge,L., Beaucage. *et al.* (eds), *Current Protocols in Nucleic Acid Chemistry*, Chapter 17, Unit 17 13.
79. Wu,S., Murai,S., Kataoka,K. and Miyagishi,M. (2008) Yin Yang 1 induces transcriptional activity of p73 through cooperation with E2F1. *Biochem. Biophys. Res. Commun.*, **365**, 75–81.
80. Wang,C.C., Tsai,M.F., Dai,T.H., Hong,T.M., Chan,W.K., Chen,J.J. and Yang,P.C. (2007) Synergistic activation of the tumor suppressor, HLJ1, by the transcription factors YY1 and activator protein 1. *Cancer Res.*, **67**, 4816–4826.
81. Lee,M.H., Lahusen,T., Wang,R.H., Xiao,C., Xu,X., Hwang,Y.S., He,W.W., Shi,Y. and Deng,C.X. (2011) Yin Yang 1 positively regulates BRCA1 and inhibits mammary cancer formation. *Oncogene*, June 13 (doi:10.1038/onc.2011.217; epub ahead of print).